fire

MDPI

Article

The Construction of Probabilistic Wildfire Risk Estimates for Individual Real Estate Parcels for the Contiguous United States

Edward J. Kearns [1,*], David Saah [2], Carrie R. Levine [2], Chris Lautenberger [3], Owen M. Doherty [4], Jeremy R. Porter [1], Michael Amodeo [1], Carl Rudeen [2], Kyle D. Woodward [2], Gary W. Johnson [2], Kel Markert [2], Evelyn Shu [1], Neil Freeman [1], Mark Bauer [1], Kelvin Lai [1], Ho Hsieh [1], Bradley Wilson [1], Beth McClenny [4], Andrea McMahon [2] and Farrukh Chishtie [2]

[1] First Street Foundation, Brooklyn, NY 11201, USA
[2] Spatial Informatics Group, Pleasanton, CA 94566, USA
[3] Reax Engineering, Berkeley, CA 94704, USA
[4] Eagle Rock Analytics, Sacramento, CA 95820, USA
* Correspondence: ed@firststreet.org

Abstract: The methodology used by the First Street Foundation Wildfire Model (FSF-WFM) to compute estimates of the 30-year, climate-adjusted aggregate wildfire hazard for the contiguous United States at 30 m horizontal resolution is presented. The FSF-WFM integrates several existing methods from the wildfire science community and implements computationally efficient and scalable modeling techniques to allow for new high-resolution, CONUS-wide hazard generation. Burn probability, flame length, and ember spread for the years 2022 and 2052 are computed from two ten-year representative Monte Carlo simulations of wildfire behavior, utilizing augmented LANDFIRE fuel estimates updated with all the available disturbance information. FSF-WFM utilizes ELMFIRE, an open-source, Rothermel-based wildfire behavior model, and multiple US Federal Government open data sources to drive the simulations. LANDFIRE non-burnable fuel classes within the wildland–urban interface (WUI) are replaced with fuel estimates from machine-learning models, trained on data from historical fires, to allow the propagation of wildfire through the WUI in the model. Historical wildfire ignition locations and NOAA's hourly time series of surface weather at 2.5 km resolution are used to drive ELMFIRE to produce wildfire hazards representative of the 2022 and 2052 conditions at 30 m resolution, with the future weather conditions scaled to the IPCC CMIP5 RCP4.5 model ensemble predictions. Winds and vegetation were held constant between the 2022 and 2052 simulations, and climate change's impacts on the future fuel conditions are the main contributors to the changes observed in the 2052 results. Non-zero wildfire exposure is estimated for 71.8 million out of 140 million properties across CONUS. Climate change impacts add another 11% properties to this non-zero exposure class over the next 30 years, with much of this change observed in the forested areas east of the Mississippi River. "Major" aggregate wildfire exposure of greater than 6% over the 30-year analysis period from 2022 to 2052 is estimated for 10.2 million properties. The FSF-WFM represents a notable contribution to the ability to produce property-specific, climate-adjusted wildfire risk assessments in the US.

Keywords: fire model; property-level; climate; fuels; ignition

Citation: Kearns, E.J.; Saah, D.; Levine, C.R.; Lautenberger, C.; Doherty, O.M.; Porter, J.R.; Amodeo, M.; Rudeen, C.; Woodward, K.D.; Johnson, G.W.; et al. The Construction of Probabilistic Wildfire Risk Estimates for Individual Real Estate Parcels for the Contiguous United States. *Fire* **2022**, *5*, 117. https://doi.org/10.3390/fire5040117

Academic Editor: Alistair M. S. Smith

Received: 13 June 2022
Accepted: 7 August 2022
Published: 15 August 2022

1. Introduction

The threat of increasing wildfire risk across the United States has been described by a number of studies that discuss both the increasing incidence of wildfire and the increasing threat to forests and communities [1–3]. The implications of this growing risk threaten the economic stability, natural resources, and quality of life for the affected communities and local residents, and there are a number of resources (e.g., https://wildfireresearchcenter.org/, accessed on 13 June 2022; https://wildfirerisk.org/, accessed on 13 June 2022) now available

to assist communities in meeting those growing risks. Westerling et al. [2] report that land management costs already exceeded USD 1 billion in costs nearly 10 years ago; however, a report from the Bureau of Land Management (BLM) and the Western Forestry Leadership Coalition (WFLC) highlighted the fact that this direct cost is simply a fraction of the larger economic costs of wildfires [4]. The WFLC report highlighted the fact that, beyond the direct dollars spent on land management and suppression, there are additional direct costs (such as firefighting crews), indirect costs (extensive and long-term implications of lost tax revenue, land recovery, and dips in property value), rehabilitation costs (watershed restoration, short term emergency loans, etc.), and additional uncharacterized costs (including human costs). The report estimates that the cost of wildfires reported through direct costs may only account for about 3% of all costs incurred from wildfires. In fact, NOAA reports over USD 79.8 billion in costs associated with the occurrence of wildfires between the most recent 5-year period of recorded events (2018 and 2021), not accounting for much of the cost associated with land management or long-term indirect and additional costs [5]. While the costs of wildfires have been exceedingly high in recent years, it is also growing at a rate that indicates its increasing impact on communities in the US, with the cost of the preceding 5 years of economic damages totaling only USD 8.5 billion (2012–2016) [5]. This increase in damages is nearly 10-fold and represents the growing risk to communities, and residents in those communities. A number of commercial fire risk products have been developed and are in wide use in the insurance industry (e.g., Verisk's "FireLine" https://www.verisk.com/siteassets/media/downloads/underwriting/location/location-fireline.pdf, accessed on 1 June 2022), but these are statistically based solely upon past fires and related damages.

The growing risk has been linked to a series of different drivers in the literature. Some explanations have drawn on anthropogenic changes in industry-associated latent consequences, such as forest regrowth following a decline in logging in the late 19th century, which allowed for structural changes to the biomass (fuels) in those areas driven by the lack of the natural regulation from regularly occurring fires [2]. Competing explanations focus on the impact of variability in climate conditions associated with the increasing risk of wildfires, including increasing variability in moisture conditions, increasing drought frequency, and warming temperatures [6]. Finally, these explanations are further compounded by the fact that the areas most at risk of wildfires in direct relation to residential land uses have grown extensively in recent years [7]. This interface, referred to as the wildlands–urban interface (WUI), has shown significant growth in the last 20 years, with Radeloff and colleagues [7] reporting about an 8% growth in WUI area and a nearly 35% growth in population and housing units. In total, the research reports that half of all homes built in the 1990s, and about 40% in the 2000s, were built in the WUI. Recent statistical analyses at the property level have shown that 97% of home losses are found in the WUI [8]. Such rapid growth in high-risk areas means that even more properties are at risk of wildfire. Beyond the impact on magnitude, the larger WUI populations simply mean there is more opportunity for fire as the vast majority are ignited by human cases [9].

In response to the need to respond to this growing nationwide risk at the community level, the U.S. Federal Government supported the creation and publication of the publicly available Wildfire Risk to Communities (hereafter WRC; see WildfireRisk.org) [10], which conveys the relative risk for communities based on a 270 m horizontal resolution analysis. The tool is primarily intended to provide insight for community level wildfire solutions in a way that allows for communities to understand their relative risk comparatively with other areas, so that resources can be allocated in a measured and efficient way, with the goal of combating economic and human loss from wildfires. Wildfire Risk to Communities' estimates are based on fire simulations that incorporate the US Forest Service's 2014 Landscape Fire and Resource Management Planning Tools database v2.0.0 [11], with some modifications (Smail, personal comm. 2021), which provides open data describing the composition and state of fuels across the contiguous United States (CONUS). However, WRC's focus is on community risk and actions to reduce those risks, and the metrics computed

are not focused on individual properties and homes, nor does WRC include the impacts of climate change on future risk.

The development of the WRC tool served as a milestone in giving communities the ability to assess risk in their area and plan for resource allocation in relation to that risk. However, the developers of the tool acknowledge that it is a community level tool and should be used for community level purposes. This research aims to build upon the wildfire community's considerable research on wildfire risk modeling [12], and to complement the WRC community level tool with a high-resolution model developed specifically for the property level at a national scale, the First Street Foundation-Wildfire Model (FSF-WFM). Given the increase in wildfire occurrence and the subsequent economic consequences [13], there remains a need to quantify the probable changes in wildfire exposure for US property owners and residents to provide to them with an improved awareness of their specific, property-level wildfire risk now and their expected risk in the future. The use of wildfire hazard estimates to provide property-level vulnerability estimates has been demonstrated in numerous studies, e.g., [14,15]. As the number of communities in the built environment suffering extensive losses grows (e.g., losses in the WUI exemplified by Gatlinburg, TN 2016; Paradise, CA 2018; Grand County, CO 2020; Boulder County, CO 2021), there is also a recognized need to describe the spread and risk of wildfire specifically within the WUI [16]. The development of such a model is based on the unique risk each individual property faces, based on property-level characteristics, and can be scaled nation-wide to provide homeowners with mitigation solutions, such as those included in the "resilience pathways" described in [17].

Building upon the WRC approach, the LANDFIRE database, climate projections, and existing open-source fire behavior models, the remainder of this document is designed to provide a transparent understanding of the framework and methodology that went into the development of the property-level wildfire model, taking an open science approach (https://earthdata.nasa.gov/esds/open-science, accessed on 13 June 2022). This study does not attempt to provide quantitative comparisons between the outputs of the FSF-WFM and the WRC approaches. While comparisons may be useful in understanding the nuances of the fuels used and model implementations, any direct quantitative estimates of the differences are difficult to interpret, not just due to those differences, but also because the models were developed with different purposes in mind. Direct quantitative comparisons with the aforementioned property-level statistical models typically used in insurance applications may be useful, since they are more similar in purpose, but due to the proprietary nature of and costs associated with those models' outputs, the authors do not currently have access to those outputs at a sufficiently large scale to conduct such a comparison. Any such comparisons of results may be the subject of a future study, but would specifically be a comparison of methodological differences of scale and purpose versus a comparison of accuracy of the models. To that point, the model described in this paper is specifically designed to measure property risk and should be thought of as complementary to the larger community risk products.

2. Model Development

The FSF-WFM approach is based on the application of a fire behavior model to explore the incidence, severity, and probability of wildfires that occur at a property-level resolution across CONUS. This general approach has been shown to be useful at large scales in the aforementioned WRC using FSim [18], and on regional scales, such as the use of WyoFire [19]. Here, we use an open-source wildfire behavior model, ELMFIRE (Eulerian Level Set Model of Fire Spread), which has likewise been shown to produce useful results in this type of application [20], but also extends its use to estimate future wildfire hazards based on climate predictions.

The development of the FSF-WFM includes a series of steps associated with the integration of fuels, fire weather, and ignition locations into ELMFIRE. While each of these

components will be explained in detail below, a definition/purpose of each component as they relate to the wildfire model is provided here for context.

- Fuels: estimation of the fuels that support wildfires across the US at 30 m horizontal resolution, including assembly of new fuel estimates updated with disturbance descriptions for the previous 10 years and the conversion of buildings within the WUI into a burnable fuel type that allows the appropriate progression of wildfire throughout the WUI in the fire behavior model.
- Fire weather: assembly of the weather data to drive the fire behavior model under a representative range of fire weather conditions for 2022 and 2052. Fire weather was derived from the National Oceanic and Atmospheric Administration's (NOAA's) surface weather reanalysis for 2011–2020 to create the 2022 hazard layers, and was driven by the same time series in 2052 with air temperature, precipitation, and humidity scaled to 2052 conditions, as represented by downscaled International Panel on Climate Change (IPCC) climate model ensemble results.
- Ignition locations: identification of the likely ignition locations, temporal fire occurrence patterns, and conditions most likely for fire spread for future wildfires.
- Fire behavior model: application of a fire incidence and landscape behavior model across the contiguous United States in a Monte Carlo simulation to build probabilistic estimates of 2022 and 2052 wildfire hazards in terms of burn likelihood, fire intensity, and spread of embers at 30 m horizontal resolution.

The resulting wildfire hazards product is based on the data sources listed, which were used to update the data to May 2021 (see Appendix A).

2.1. Fuels

The wildfire hazard estimate is heavily dependent upon estimates of the type, quantity, age, and condition of the combustible fuels across the US. Version 2.0.0 of the canonical U.S. Forest Service (USFS) LANDFIRE [11] fuels dataset at 30 m horizontal resolution is utilized as a baseline for provision of this fuel information, and is updated to characterize the risks in the present through the inclusion of all known disturbances from May 2021 to create a current fuels layer that is useful for assessing wildfire risk for the year 2022. One must note that not all disturbances were able to be adequately documented or described, and different US states exhibit different levels and styles of reporting. States with the highest fire risk in the Western and Southeastern US (e.g., California, Oregon, Arizona, Colorado, Washington, Idaho, and New Mexico) were prioritized to ensure their adequate inclusion in this study. These disturbances were incorporated as changes to surface and canopy fuels by modifying the geographically referenced LANDFIRE classifications, and include recent wildfires, prescribed burns, harvests, and other forest management practices, as reported by the data sources listed in Appendix B. Modification of the fuel descriptions was carried out in accordance with the LANDFIRE fuel classes and methodologies, and is congruent with the LANDFIRE disturbance code schema, which consists of thematic three-digit code values corresponding to disturbance type, severity, and time since disturbance, respectively, per the LANDFIRE Fuel Disturbance Attribute Data Dictionary [21]. A representation of the processes is shown in Figure 1 that describes the methods used to create the fuels estimate for this study.

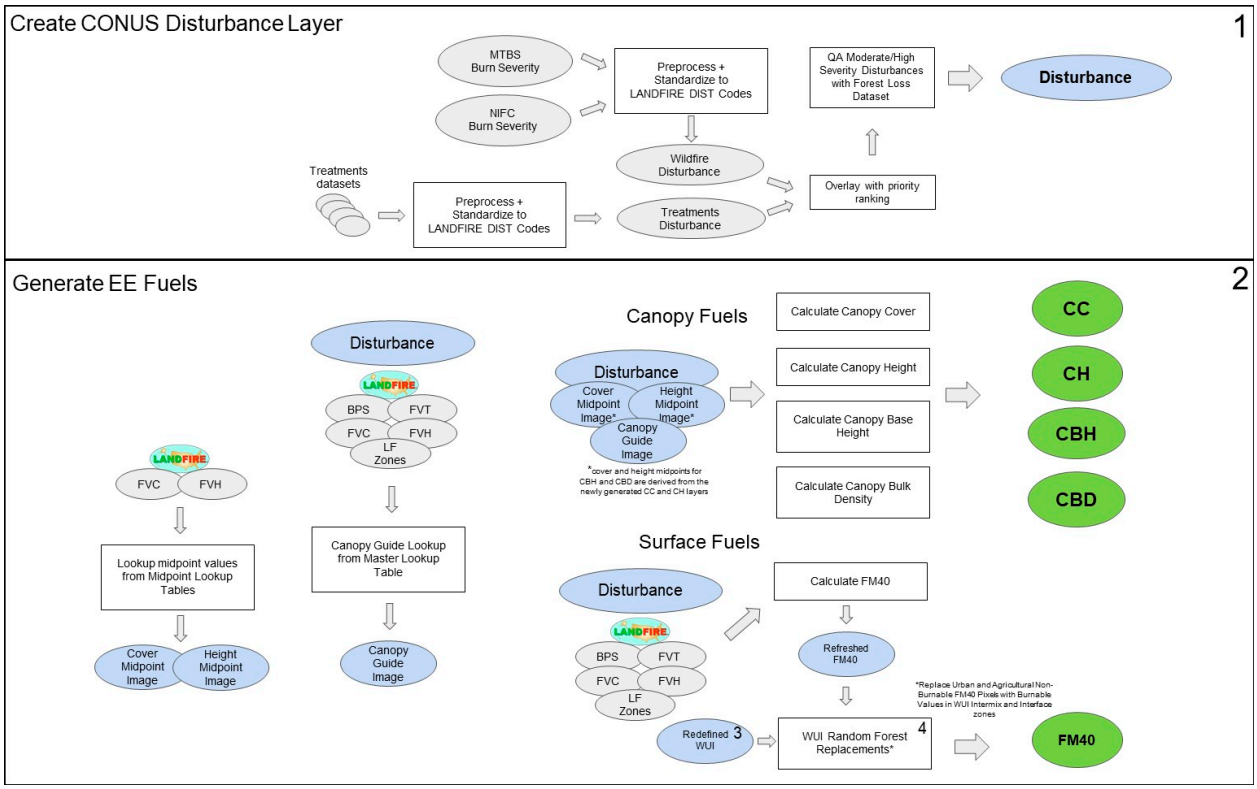

Figure 1. The modifications of the LANDFIRE v2.0.0 fuels (LF), including use of disturbance data (FVC—fuel vegetation cover; FVH—fuel vegetation height; FVT—fuel vegetation type; BPS—biophysical settings) to modify surface (FM40) and canopy fuel classes (canopy cover—CC; canopy height—CH; canopy base height—CGH; canopy bulk density—CBD), and the replacement of non-burnable fuel classes in the WUI with fuel classes that were found to approximate observed fire behavior in past WUI fires. Computation was performed using Google Earth Engine (EE). This figure represents steps 1 and 2 in the fuel methodology; steps 3 and 4 are included in Figure 4.

2.1.1. Disturbances

Disturbances from wildfires across CONUS were incorporated by using data shared by the Monitoring Trends in Burn Severity (MTBS) [22] program, which maps the burn severity and extent of large fires across all lands in the US. At the time of analysis, the MTBS dataset included fires of an area larger than 500 acres through 2019. Therefore, for the year 2020, the MTBS dataset was augmented with data from all fires of size <500 acres from the National Interagency Fire Center (NIFC).

To ensure the consistency of fire severity characterizations between the MTBS and NIFC datasets, burn severity was informed by calculating the normalized burn ratio (NBR) [23] for one pre-fire and one ninety-day-window post-fire cloud-filtered composite image corresponding to each fire. The pre-fire NBR was then subtracted from the post-fire NBR to create the relative difference normalized burn ratio (RdNBR) index [23]. "Miller's threshold" [23] was then applied to the RdNBR image to create a five-class burn severity classification.

For non-wildfire disturbances, including harvest, fuel mitigation treatments, and prescribed burns, there are no uniform naming or reporting conventions for forest management practices across the U.S. and the quality of data entry varies considerably from state to state. To ensure that every feature is assigned a standardized disturbance class, all unique treatment names from every dataset were compiled for review by forestry field experts who are included in the authorship of this paper. Each unique disturbance name in the document was assigned a LANDFIRE disturbance type, and assigned the appropriate three digit LANDFIRE disturbance code that captures disturbance types, severity, and time

since disturbance. A distribution associated with the types and severity of disturbances is reported in Table 1.

Table 1. Distribution of disturbance types and severity.

Disturbance Type	**%**
Fire	92.8%
Mechanical add	0.2%
Mechanical reduce	5.8%
Other	1.2%
Disturbance Severity	**%**
Low	65.0%
Medium	20.2%
High	14.8%

The disturbance types most frequently found in our dataset and listed in Appendix B were fire (disturbance type 1), mechanical add (disturbance type 2, when fuels are mechanically mowed or chipped and transitioned to surface fuels), and mechanical remove (disturbance type 3, when fuels are removed via cutting, felling, burning, or harvest). We assigned a disturbance type of "other" (disturbance type 8) to chemical treatments and grazing. We excluded treatments or activities included in the datasets that would not have impacted fuels (including but not limited to seeding, habitat restoration, and invasive species removal). Treatment disturbances, such as hand thinning, piling, prescribed fire, and other treatments where canopy cover is not altered were assigned a disturbance value of 1 (low severity); mechanical thinning and harvest were assigned a disturbance value of 2 (medium severity); and clear cuts were assigned a disturbance value of 3 (high severity). For wildfire disturbances, we followed the MTBS conventions, whereby fire severity class 2 are low severity, 3 are medium severity, and 4 are high severity classifications. Classes 1 (unburned/unchanged) and 5 (increased greenness) were considered undisturbed. The code for time-since-disturbance was determined based on the year of treatment and the LANDFIRE zone. Time-since-disturbance was categorized as 1 (disturbances that occurred in 2020), 2 (disturbances that occurred in 2015–2019), and 3 (disturbances that occurred in 2011–2014). Due to differences in overall fire risk topographies, for disturbances that occurred in the LANDFIRE Southeast Super Zone (Zones 46, 55, 56, 58, and 99), the time-since-disturbance categories are 1 (disturbances that occurred in 2020), 2 (disturbances that occurred in 2017–2019), and 3 (disturbances that occurred in 2011–2016). Finally, the treatment and wildfire layers were combined into a single disturbance layer using a priority ranking ruleset informed by LANDFIRE analysts (Smail, personal comm. 2021) to ensure the most fuels-relevant disturbance value is assigned in cases of spatial overlap.

Validation with the CONUS scale is most practically accomplished with remote sensing techniques. The Hansen Global Forest Change dataset [24] provides a 'loss year' band that represents the year(s) when there was detectable canopy loss during the period 2000–2020 at the 30 m per pixel scale. We leveraged this band to create a forest loss bitmask for 2011–2020 and applied it to screen our final aggregate disturbance layer to remove false positives of moderate and high severity harvest [24].

2.1.2. Fuel Layers

Using LANDFIRE v2.0.0 as the base, four canopy fuel layers (canopy cover, canopy height, canopy base height, canopy bulk density) and one surface fuel layer (40 Scott and Burgan Fire Behavior Fuel Model, hereafter FM40) [25] were generated with an effective year of 2021 for use as inputs into the fire models. Fuels were only transitioned in areas that were disturbed between 2011 and 2020. Initial layers that represented lookup rulesets in the LANDFIRE Total Fuel Change Tool (LFTFCT) database were generated. First, canopy cover and height midpoint layers are derived from the LANDFIRE Fuel Vegetation Cover

(FVC) and Fuel Vegetation Height (FVH) rasters based on the LFTFCT lookup table values. Next, using the new updated disturbance layer, a canopy guide layer was generated by using the LFTFCT master lookup table applied to unique combinations of the disturbance code, biophysical Settings (BPS), fuel vegetation cover (FVC), fuel vegetation height (FVH), and fuel vegetation type (FVT). The four canopy fuel layers are then generated using the following regression equation:

$$Canopy\ Fuel = C_X + H_y + b \quad (1)$$

where C is the canopy cover midpoint, H is the canopy height midpoint, x and y are the scale factors, and b is an intercept value derived from a lookup of unique disturbance code and FVT combinations from the LFTFCT lookup table. For canopy cover and canopy height regressions, the cover and height midpoint values are derived from the initial FVC and FVH midpoint layers described above, while for canopy base height and canopy bulk density, the midpoint values are derived from the new canopy cover and height layers that were generated in the step described above. Additionally, canopy bulk density uses a ruleset to create two stand height coefficients from the canopy height midpoint value for pixels following the rules described in [26]. Each canopy fuel regression output is post-processed to ensure values are within the LFTFCT's valid value range (CC: 0–95; CH: 0–510; CBH: 0–100; CBD: 0–45), scaled properly, and binned, if necessary, to defined midpoint values [21]. Finally, the LFTFCT canopy guide layer is applied to each layer using rulesets based on canopy cover thresholds [21].

The FM40 surface fuel estimates are generated in the same way as the canopy guide, using the LFTFCT master lookup table applied to unique combinations of the disturbance code, BPS, FVC, FVH, and FVC. Products generated include the necessary LANDFIRE fuel and vegetation datasets for the workflow described here, derived fire severity, canopy cover and canopy height midpoint, as well as disturbance estimates. Included with the 2021 fuel profile used in this study are the following five updated 2021 fuel layers: FM40, canopy cover (CC), canopy height (CH), canopy base height (CBH), and canopy bulk density (CBD). Figure 2 highlights the spatial location of the canopy and surface fuel updates across the CONUS, with Figure 3 highlighting the update of surface fuels in a more local context.

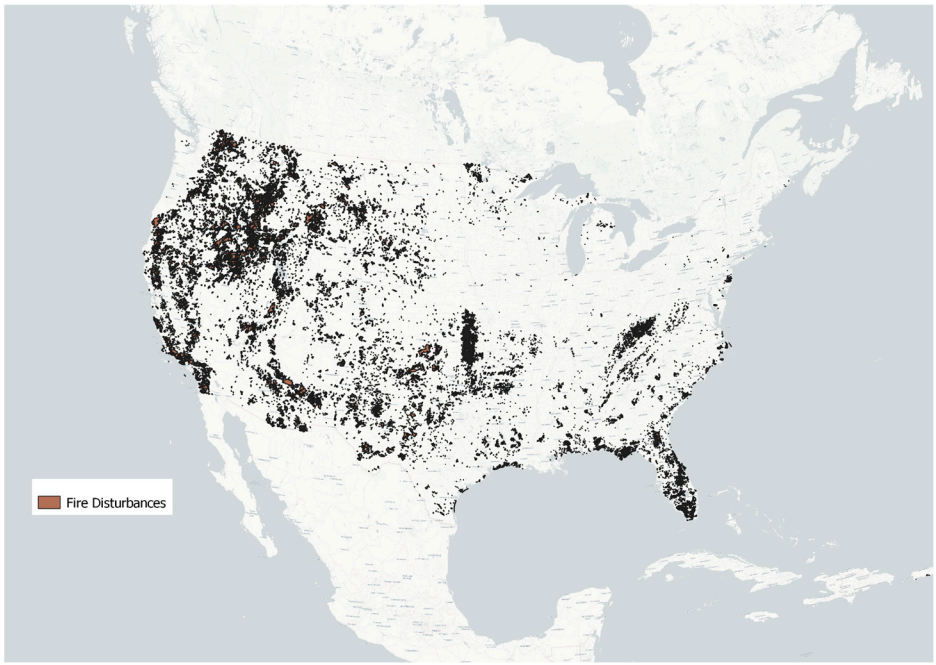

Figure 2. Disturbances: locations of updated canopy and surface fuels.

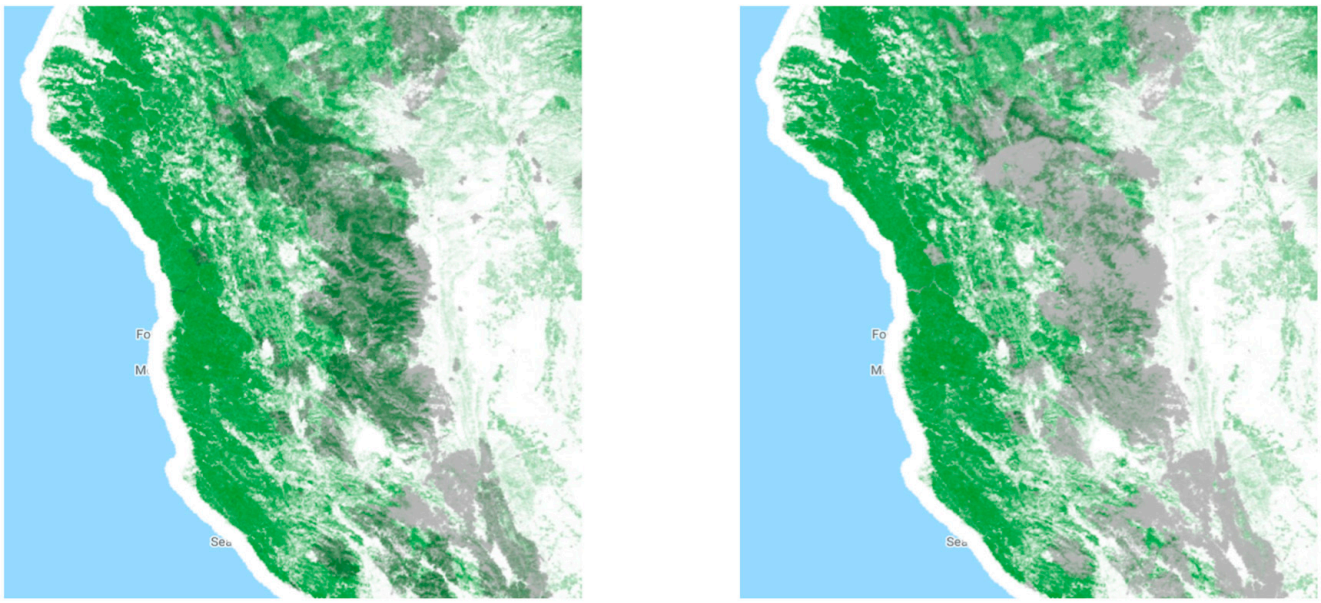

Figure 3. Modified surface fuel estimates: (left) LANDFIRE 2016 canopy cover (green) and identified disturbances 2017–2020 (gray) are shown. (Right) new canopy cover estimates (green) are reduced in disturbed areas.

2.1.3. WUI Surface Fuel Updates

Typically, homes and other buildings in the built environment, including the WUI, are classified as non-burnable fuels within LANDFIRE. However, in order to allow the estimate of wildfire hazards within the WUI under the full range of fire weather conditions, those properties within the WUI need to be replaced by a burnable fuel estimate to permit the wildfire behavior model to estimate how wildfire could move through the WUI more accurately.

The first step of developing the WUI fuel model was to derive a current map of WUI areas. WUI areas are defined by the following two factors: building density and the distance from wildland vegetation [27]. We used the 2016 NLCD existing vegetation cover layer to identify areas of wildland vegetation, and derived our own building-density layer from MapBox building footprints (Appendix A), following evidence from Caggiani et al. [8] that such higher-resolution analyses enable more precise evaluations of wildfire risks. The WUI influence zone, WUI intermix, and WUI interface layers were defined as the following [16]:

Influence zone is >75% land coverage of wildland vegetation within 1 mile of a residence.
Intermix is >1 residence per 40 acres and groups of residences larger than 50 acres, with >50% land coverage of wildland vegetation.
Interface is defined as >1 residence per 40 acres and groups of residences larger than 50 acres, with <50% land coverage of wildland vegetation, and within 1 mile of wildland vegetation.

Non-burnable pixels were converted to a burnable FM40 fuel type in the WUI intermix and interface only, as much of the WUI influence zone is already estimated as burnable in LANDFIRE and does not need to have non-burnable cells converted to burnable cells to enable the fire behavior model in those areas. Any unnecessary conversions within the influence zone could potentially result in biased fire behavior by changing the FM40 fuel types in those areas.

Properties within the WUI with a non-burnable classification in the 2021 fuel profile were replaced by an effective fuel type by estimating it from a statistical analysis of 549 historical fire perimeters in the WUI from 2014–2019 (see Appendix C). These past fires were used to train a random forest machine learning algorithm to predict the appropriate fuel classification. One must note that the fuel layers do not take into account fuel estimates for the structures themselves in the WUI that could lead to increased house-to-house ignition probability; such an approach could be incorporated into a future effort. To convert non-burnable pixels in the WUI intermix and interface to allow the fire behavior model in those regions, we used a machine learning approach, as described below.

The 2021 FM40 fuel types derived in the fuel workflow (see Figure 1) described above are used as the response variable. The training and testing datasets were composed of pixels in the WUI intermix and interface that were within the fire perimeters from our disturbance dataset (2011–2020) or within a 1 km buffer around the fire perimeter, in order to capture areas that remained unburned in those incidents. Other variables included vegetation products from LANDFIRE v2.0.0 [11], Landsat data derived from 4-month composites encompassing each training fire's ignition date (coastal, blue, green, red, NIR, NDVI, SWIR1, SWIR2, NDVI, MNDWI, BAI), GRIDMET data derived from 1-month composites encompassing each training fire's fire ignition date (tmin, tmax, fm1000, vs, mndwi, erc, bi), topography variables from USGS (slope, elevation, aspect), building density per 1 km^2, the number of structures destroyed per fire, and fire severity. A random-forest model was trained only on burnable FM40 categories. The prediction area was limited to 2021 FM40 urban/developed (FM40 class 91) and agricultural (FM40 class 93) land in the WUI intermix and interface. We ran a stratified k-fold cross validation training using 10 folds for each dataset, with the training data split 80−20% in each run. The best model had a k-fold training accuracy of 73.0%, with a mean precision (true negative rate) of 76.4% and a mean recall (true positive rate) of 73.0%. Overall, k-fold training had a mean model accuracy of 71.2% (68.7–73.7% confidence interval). The overall training accuracy was 96.9%, with a training Kappa coefficient of 96.8%. For model testing, 30% of the sampled data was withheld. The independent validation dataset showed 71.7% accuracy, with a testing Kappa coefficient of 73.0%. A framework for documenting the classification process to replace non-burnable FM40 classes with burnable classes in the newly defined WUI is presented in Figure 4, with feature importance highlighted in Figure 5.

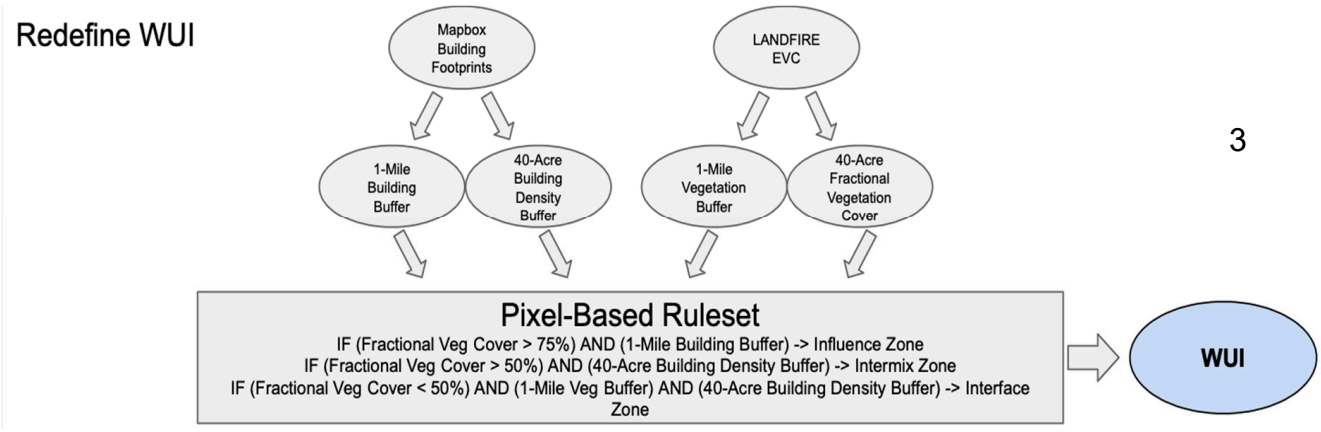

Figure 4. *Cont.*

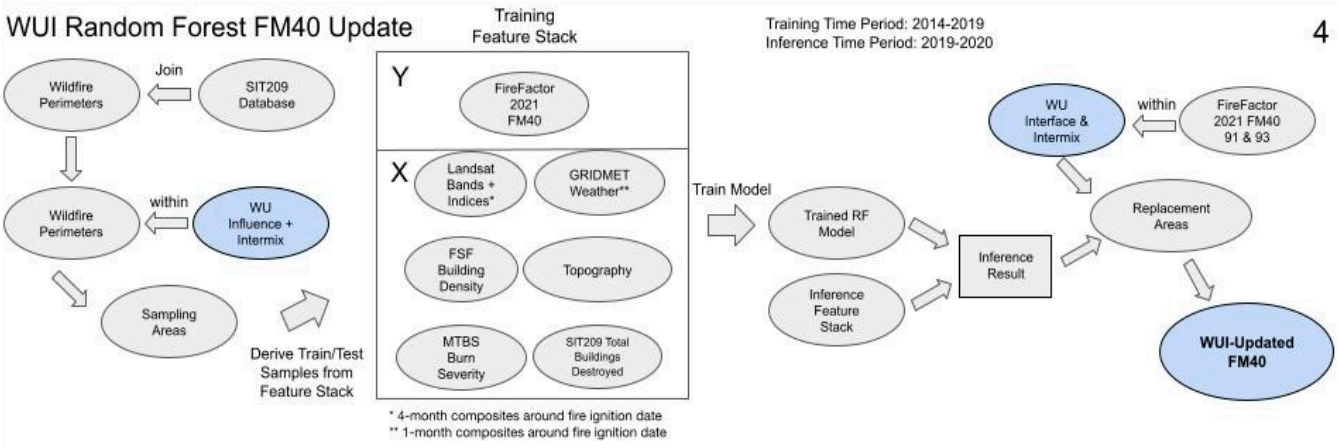

Figure 4. Random forest model training and classification to replace non-burnable FM40 classes with burnable classes in the newly defined WUI.

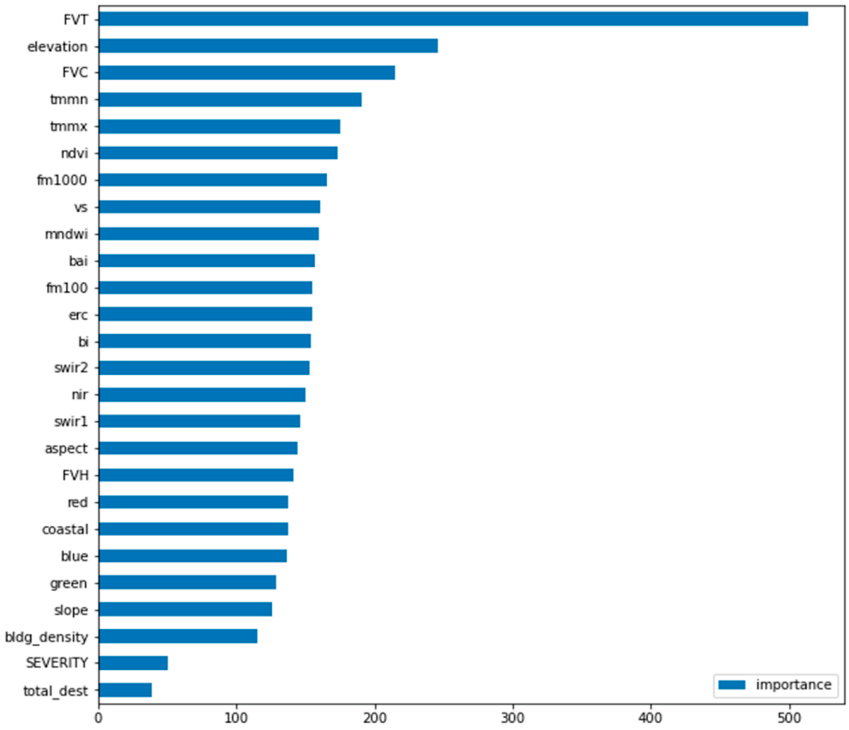

Figure 5. WUI FM40 random forest importance values.

Overall, the vegetation, topographic, and weather variables had higher importance than the fire-related or building density-related variables in the model (Figure 5). In general, non-burnable WUI intermix and interface pixels were frequently replaced with grass or grass-shrub fuel types (FM40 classes 101 and 121, and occasionally 103 in the southeast and 183 in the mid-Atlantic). The predicted pixels were replaced in the 2021 FM40 fuel layer to create the final 2021 FM40, with the surface fuel model updated for both disturbances and WUI areas (see Figure 6, for example).

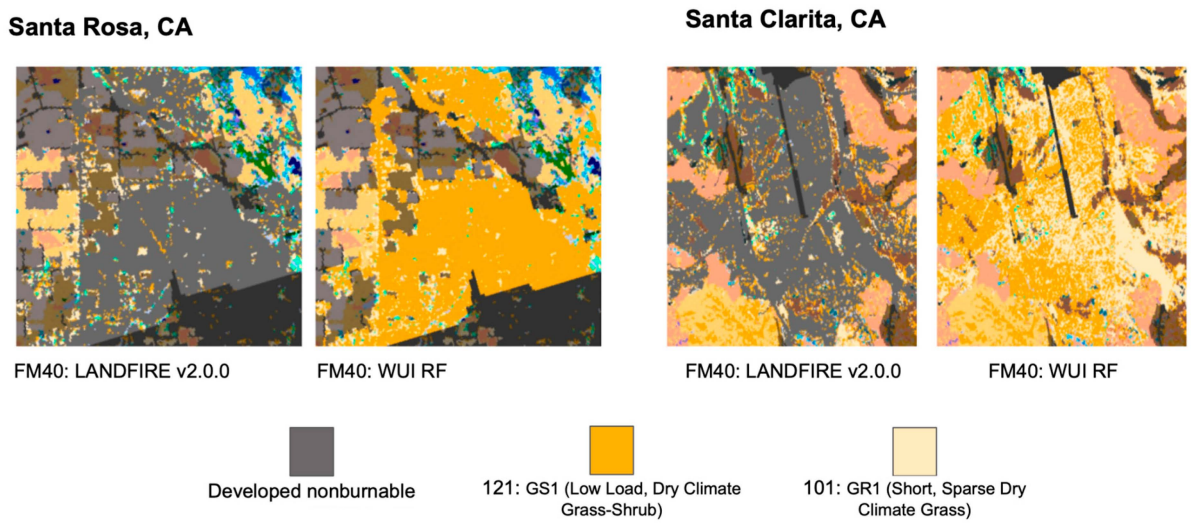

Figure 6. Classification of building structures from unburnable to burnable fuel types.

2.1.4. Vegetation Changes and Impacts on Fuels

Changes in the composition and volume of vegetation due to climate change's impacts have been discussed in depth by a number of researchers, including Westerling et al. [2], Radeloff et al. [7], Krawchuk et al. [28], and their importance to estimates of fire intensity has been discussed more recently in a review article by Bowman et al. [29]. These studies typically examine those vegetative changes over time periods of 75 to 150 years, while the current study is focused on 30 years only. To investigate the size and scope of vegetation changes on a 30-year time period at 30 m horizontal resolution, we originally planned to utilize the Land Use and Carbon Scenario Simulator [30], a Monte-Carlo based state-and-transition simulation model, to project changes to 14 carbon pools from 2021–2051. While we observed statistically significant changes in above ground modeled carbon pool volumes over 30 years across CONUS, we struggled to accurately translate this from those carbon pools to the canopy and surface vegetation classes needed to drive the fire behavior model we employ in this study. While research continues on this and several alternate ways of estimating the vegetation and fuel changes anticipated across CONUS over 30 years in a changing climate, we have elected to hold the fuel constant between the 2022 and 2052 simulations for the purposes of this study. Future wildfire exposure estimated by the model described in this study will then be independent of future vegetation changes, and will depend only on the future weather impacts on the fuel conditions and fire behavior alone.

3. Fire Weather and Climate Change

The primary inputs needed to drive the fire spread model are fuels, topography, and weather. This section details the integration of climate weather into the development of the larger FSF-WFM. The weather that can drive the growth and distribution of wildfire can be separated into the following two categories: (1) the weather before the onset of a wildfire that impacts fuel condition by making the fuels drier or wetter, and (2) the 'fire weather' that occurs at ignition, which can increase intensity and drive fire across the landscape. To represent a wide range of possible weather-driven fire conditions across the landscape within the simulations employed here, we used a decade of high spatial and hourly resolution weather data. Wind speed and direction, relative humidity, and temperature inputs were assembled from the Real Time Mesoscale Analysis (RTMA) dataset [5], which provides hourly estimates of sensible weather variables on a 2.5 km grid for CONUS. The RTMA surface weather data reanalysis from 2011–2020 was augmented by Oregon State PRISM (Parameter-elevation Regressions on Independent Slopes Model) [31] precipitation data to fill in gaps in the RTMA data. Ten years was chosen to represent a wide range of weather conditions, while overlapping the time period for which the fuel state is represented (i.e.,

LANDSFIRE 2016 augmented to 2020). While a 20- or 30-year time series would provide a more complete sampling of the possible meteorological conditions, the 10-year time series does include multiple La Niña and El Niño phases and allows for the computations to be completed in a reasonable span of time, given the available resources. Additionally, since this study does not set out to replicate or predict anomalously large or intense fires (e.g., plume fires) in a deterministic sense, the Monte Carlo approach used will deemphasize those extreme or infrequent conditions and instead emphasizes the much more frequent medium-large fires (i.e., larger than those that are easily suppressed, but smaller than the rare extreme fires).

To represent the 2052 weather, we have considered the 2048–2057 time series, created by scaling the hourly 2022 RTMA time series, to forecast 2052 conditions. To do this, we used the International Panel on Climate Change's (IPCC) Fifth Coupled Model Intercomparison Project (CMIP5) ensemble results [32] following the Representative Concentration Pathway 4.5 (RCP 4.5), as downscaled within the daily Multivariate Adaptive Constructed Analogs (MACA) v2 product [33] to represent the expected weather conditions in 2052 across CONUS. The RCP 4.5 climate model results were chosen to be relatively conservative in outlook, and to be consistent with previous and similar work conducted for future flood risk authors [34,35].

Surface winds were held constant from the 2022 to the 2052 simulation period to preserve the realistic and high-resolution aspects of the NOAA RMTA time series in the future, to reduce uncertainties in future fire behavior and in recognition that future winds are likely to change far less significantly with climate change than other weather parameters [32,33]. The ELMFIRE fire behavior model is necessarily very sensitive to winds, and downscaled climate model results have difficulty resolving the local and orographic effects in the wind fields to a sufficient fidelity to support such fire models [36]. Even if they captured the spatial variability adequately, the high-resolution winds generated by an atmospheric model driven by boundary conditions generated from the climate model outputs would still require extensive verification and validation to be able to use them for our simulations and justify the results. Since the goal is not to recreate any particular fire event, but to use the weather time series to support a range of conditions suitable for Monte Carlo simulation, we concluded that holding the winds constant from the 2011–2020 time series to drive 2052 fire behavior would be a reasonable approach.

With winds held constant, the other 2022 weather variables underwent scaling to create a 2048–2057 hourly times series used to derive the 2052 wildfire hazards. The MACAv2 downscaled CMIP5 RCP4.5 outputs at daily resolution were used to scale the RTMA hourly time series of air temperature, relative humidity, and precipitation by computing bias adjustments between the present-day 2022 and forecast 2052 conditions (Appendix D). The biases were distributed throughout the day via gamma distribution to maintain the diurnal signal in precipitation and humidity, while allowing for the overall scaling to be representative of the climate change impacts on these variables. Extreme values in biases were adjusted inward (towards the center of the distributions) to allow for consistent statistics, while preserving the general climate variability. Air temperature adjustments at the hourly resolution were likewise adjusted with a simpler gaussian distribution that brought daily average values of the 2011–2020 RTMA hourly time series in line with the future 2048–2057 MACAv2 daily values.

The result for the 2052 weather time series is a 10-year duration, hourly resolution representation of the estimated future weather conditions at 2.5 km horizontal resolution that are characterized predominately by 1.7–2.8 deg C (3–5 deg F) average warmer temperatures across CONUS. This allows the impact of higher air temperatures from climate change on fuel conditions in 2052 to be largely isolated and evaluated, since winds and fuels are both held constant from 2022. The greatest deficiency of this approach is that it is not possible to evaluate the climate impacts of geographically coherent but temporally variable features, such as more severe or longer droughts, or greater incidences or intensities of atmospheric rivers or hurricanes. As such, these estimates are limited almost entirely to the

effects caused by higher air temperatures on fuel conditions, and so must be considered an underestimate of the total possible effects of climate change on wildfire probability. Subsequent versions of this model are intended to address these deficiencies.

4. Ignition and Spatial Fire Occurrence Patterns

One of the primary indicators of where future fires will occur is informed through historical fire occurrence data. The spatial component of the fire occurrence model is built from the Fire Occurrence Database (FOD; https://www.fs.usda.gov/rds/archive/Catalog/RDS-2013-0009.5, accessed on 1 June 2022) developed by the USDA Forest Service [37,38]. The FOD includes 27 years (1992–2018) of fire occurrence data, encompassing 2.17 million georeferenced wildfire records that total 165 million acres burned. Following the best practices for annualized burn probability modeling [18], this database was filtered to remove small fires, defined as those that are less than 100 acres (Class A, B, and C fires). We acknowledge the choice of the 100 acre cutoff is somewhat arbitrary, and different thresholds (e.g., 300 acres [18], 247 acres [39]) have been used in other research and models, but was chosen as a convenient approximation of the typical scale of wildfires whose growth are often limited by human fire suppression activities.

A recognized best practice is to develop an ignition density grid using a kernel density tool [18]. The ignition density kernel formula used (see equation below from [40]) was implemented in the wildfire behavior model to generate the ignition density grid for this work, where r is the search radius (bandwidth) and di is the distance from point i to the centroid of a given cell.

$$Density = \frac{1}{r2} \Sigma_{i=1}^{n} \frac{3}{\pi} \, x \, (1 - (\frac{di}{r})^{2}) \; for \; di < r \tag{2}$$

Modeling Temporal Fire Occurrence Patterns

The previous section describes how the spatial fire occurrence is modeled, but it does not address when large fires may occur. One of the strongest predictors of temporal occurrence of both the number of large fires and acres burned is the National Fire Danger Rating System (NFDRS) Energy Release Component (ERC) percentile based on fuel model G, or ERC(G)′ [41] (note ERC(G) refers to raw ERC values (Btu/ft2) and ERC(G)′ refers to ERC percentiles). ERC is 4% of the energy per unit area (Btu/ft2) that would be released during a fire. ERC depends on live and dead fuel loading by size class (as characterized by an NFDRS fuel model), as well as fuel moisture content of live and dead fuels. Although NFDRS fuel model G, which shows the best correlation with fire occurrence and burned area, contains loadings across all dead fuel size classes and live herbaceous/live woody loadings, it has a heavy loading in the 1000-hr size class. For that reason, ERC(G) is primarily a function of weather conditions over the preceding 45 days and can be thought of as a measure of intermediate to long-term dryness and as it is calculated solely from fuel moisture content, ERC is not a function of wind speed, slope, or spread rate.

Fire occurrence is normally assessed in terms of ERC percentile, as opposed to raw ERC (Btu/ft2), because ERC percentile shows better correlation with fire occurrence and size than raw ERC, since the same amount of precipitation that corresponds to wet conditions in one region may correspond to dry conditions in another region.

$$log_{10} \, n = 0.02768 \; \times \; ERC \; (G)\prime - 0.2333 \tag{3}$$

Figure 7 shows the number of large fires in the Western US as a function of ERC(G)′. The data in Figure 7 are demonstrably well-fit (R^2 = 0.94) by the correlation in the equation above [41], which is used in the wildfire behavior model to calculate fire occurrence from ERC(G)′.

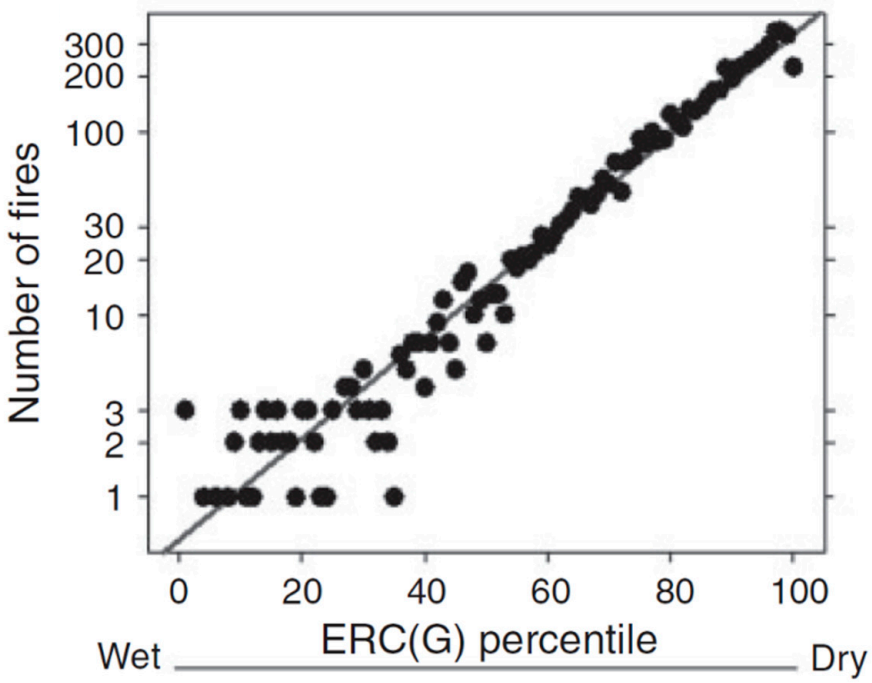

Figure 7. Number of fires in the Western US as a function of ERC(G) percentile (reproduced from Riley et al., 2013 [41]).

5. Wildfire Behavior Model

In the development of the FSF-WFM, we employed the open-source wildfire behavior model, ELMFIRE, which is a highly parallelized model that was used to both simulate fire spread and quantify the wildland fire hazard via Monte Carlo simulations. ELMFIRE is a Rothermal-based, level set model used to track boundaries across the landscape based on the numerical solutions of [42] and is fully described in Lautenberger [43].

The overall fire hazard and probability modeling methodology, as shown graphically in Figure 8 and described in this section, is based on the work of Finney et al. [44], best practices described by Scott et al. [18], and a relatively recent review of simulation-based burn probability modeling [45]. Consequently, the contribution of this work is not developing new techniques or approaches to fire probability and hazard modeling, but rather implementing computationally efficient and scalable modeling techniques based on existing fire probability and hazard modeling paradigms pioneered by the aforementioned authors. These scalable computing techniques make it possible to conduct CONUS scale fire probability and hazard simulations at 30 m resolution in a reasonable amount of time, using commodity-style computational resources. The CONUS domain was subdivided into 48 km by 48 km tiles, which were likewise surrounded by 8 similar tiles in a 3×3 grid pattern, to aid in the distributed compute workflow.

Inputs to ELMFIRE include fuels, weather time series, and ignition locations. The ignition locations were based on historical (1992–2018) fire locations described in the previous section, and limited to fire sizes of greater than 100 acres. This limitation allows the implicit inclusion of the effect of human-driven fire suppression activities in the model output to create a "real world" estimate of fire exposure—i.e., wildfires that are actively prevented from growing large. For example, the State of Rhode Island has exhibited remarkable fire suppression over the past decades and has been able to eliminate all fires over 100 acres during the 1992–2018 time period, driving the effective burn probability in Rhode Island to zero for all properties in our simulations.

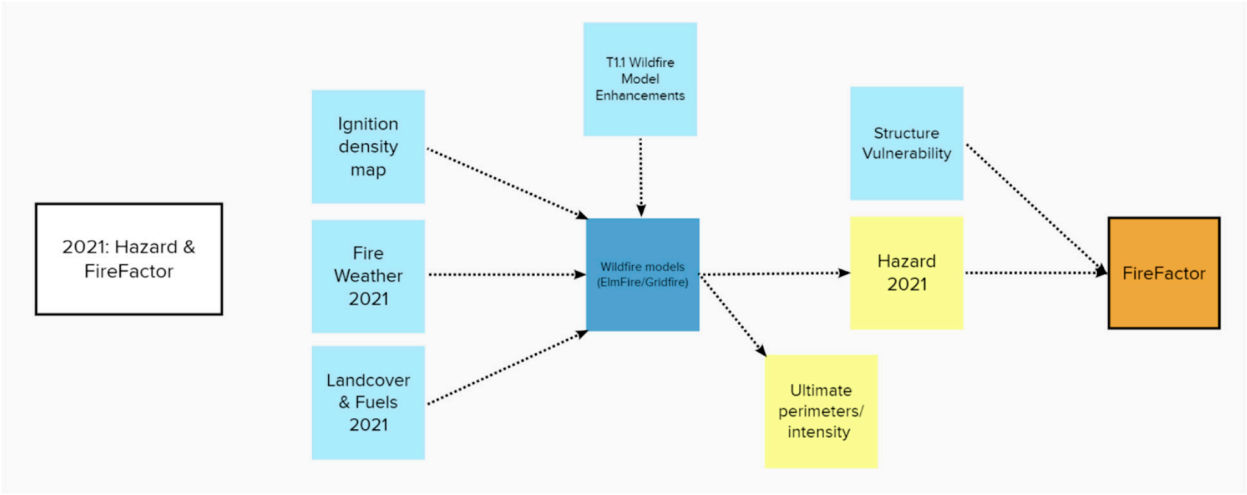

Figure 8. Wildfire behavior model, process diagram. The "fire factor" result on the right hand side is an expression of wildfire hazard as a function of burn probability, flame length, and ember presence and is available for viewing for every property in the U.S. at riskfactor.com (accessed on 8 August 2022).

For each ignition location, a weather "draw" was randomly selected for that fire that would be carried forward many hours in simulation, and could extend anywhere in the 3 × 3 (144 × 144 km) tile domain. Those simulated fires that grew to sufficient size (100 acres) were tracked and the locations, fire length, and durations were noted. This process was repeated over 100 million times, and resulted in approximately 8–10 million tracked fires of significance per simulation (2022 and 2052). The result is a statistically well-characterized set of simulated wildfires, from which the probabilistic exposure of properties and buildings to wildfire hazard based on likelihood (i.e., burn probability), flame length (i.e., intensity), and ember cast may be derived. The likelihood of a 30 m pixel burning is the number of times that the pixel had ignited over the course of all the simulations. The flame length is a measure of fire intensity, captured as binned flame lengths (see Table 2) over the distribution of all fires within the pixel, and may be expressed as the mean, median, or maximum flame length. The ember cast is a binned measure of the number of times embers, pushed ahead of a simulated fire by the fire weather time series, land in a pixel and results in an ignition of the fuels in that pixel.

5.1. Fire Spread Model

The 2D fire simulator ELMFIRE is used here to drive a stochastic fire spread analysis that is used to generate the CONUS burn probability and hazard estimates. ELMFIRE's computational engine is similar to other two-dimensional fire simulators, such as FARSITE [46], in that it calculates surface fire spread rate using the Rothermel surface spread model [47,48], assumes that each point along the fire front behaves as an independent elliptical wavelet [49], with length to breadth ratio determined empirically [48,50], simulates transition from surface to crown fire using the Van Wagner criterion [51] (with crown fire spread rates calculated from Cruz et al. [52]), and models ember-driven ignition or "spotting" as a stochastic process with lognormal spotting distance distribution [53,54]. ELMFIRE tracks the fire front using a narrow band level set method [55], a numerical technique for tracking curved surfaces on a regular grid.

Table 2. Hazards quantified by the FSF-WFM: following the ELMFIRE simulations for 2022 and 2052, the wildfire hazard for any 30 m pixel within the CONUS domain is represented by the combination of the burn probability, mean or maximum flame length (intensity), and exposure to embers.

Measure of Exposure	Description	Units
Burn probability	Likelihood that a pixel catches fire out of all the simulations normalized by likelihood of ignitions	%
Max flame length	Maximum flame length experienced at a pixel across all simulations	ft
Sum of flame length	Sum of flame length for all simulations that experience fire	ft
Mean flame length	Sum of flame length divided by times burned	ft
Binned counts of flame lengths	(0,2,4,6,8,12,20,+)	ft
Ember lux	Dimensionless number that is a proxy for the count of embers landing in a pixel. Does not reflect mass of embers, whether they are still burning, or distance traveled	<none>
Ember likelihood	Likelihood that an ember falls into a pixel across all simulations, similar to times burned	%
Max embers	Max number of embers	count

To demonstrate how ELMFIRE simulates fire spread, Figure 9 shows 24-h of fire progression from an individual ignition site. The black contour lines in Figure 9a represent the fire front position at 2-h intervals. Figure 9a also shows which parts of the burned area experienced surface fire (blue), passive crown fire (green), or active crown fire (red). Figure 9b similarly shows fire perimeter contours and flame length variation within the fire perimeter. Flame length is highest in the areas that burn as heading fires or that experience crown fire and lowest in the areas that burn as a flanking, backing, or surface fire. In this example, the fire area after 24 h of spread is approximately 560 acres.

The Monte Carlo fire spread analysis conducted here involves running millions of fire spread simulations (similar to that shown in Figure 9) sequentially over many years (2011–2021, and 2048–2057), and across all tiles in the CONUS domain. Each tile is a 144 km by 144 km tile within CONUS, consisting of a 48 km central tile surrounded by its eight neighboring tiles of the same size. For each year and tile, fuel, topography, and yearly weather, fuel moisture, and ERC percentile inputs are assembled. Starting at the beginning of the simulation year, ignition locations are determined using the spatial and temporal fire occurrence modeling techniques described earlier. Fires are ignited only in the central 48 km tile, but are allowed to spread into the adjacent eight tiles within the simulation. The progression of each fire is modeled for a randomized spread duration up to 7 days from the time of ignition, to roughly approximate the varying duration of the observed wildfires. For each pixel within the modeled fire perimeter, the burn incidence is recorded, and the binned distributions of discrete ember count and flame length are also recorded for each pixel. This ignition-burn-record process is repeated for each day in each simulation year, building up the probabilistic estimates of burn probability, flame length, and ember spread. Since fires can start in one tile and spread to adjacent tiles, each tile is post-processed concurrently with its eight neighbors.

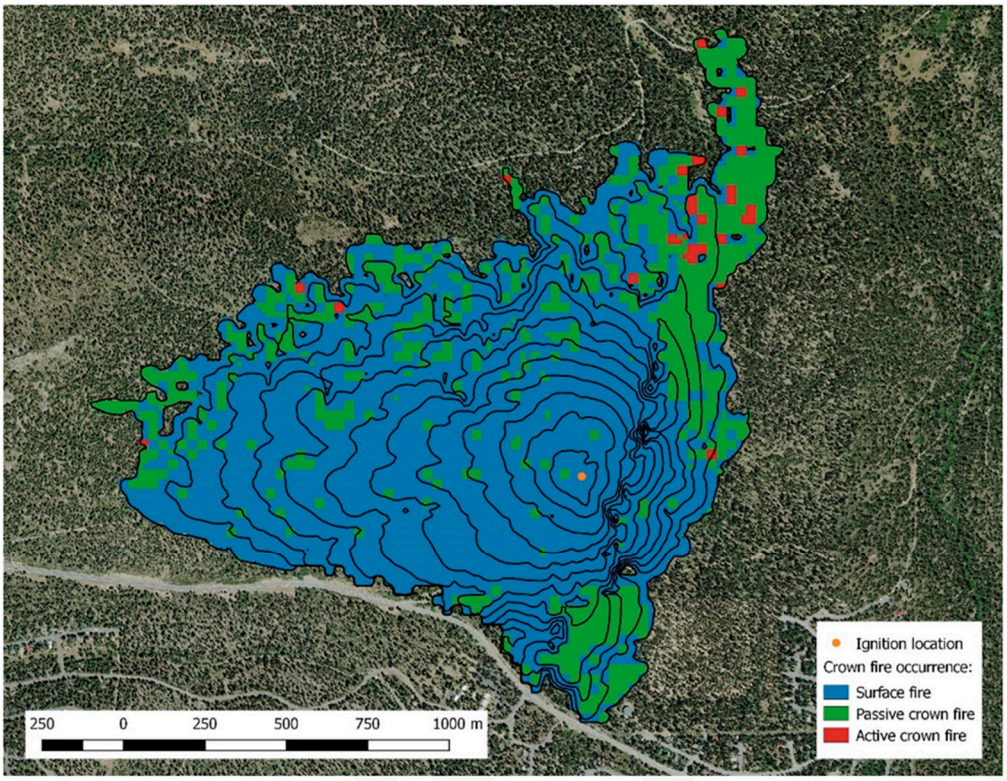

(a)

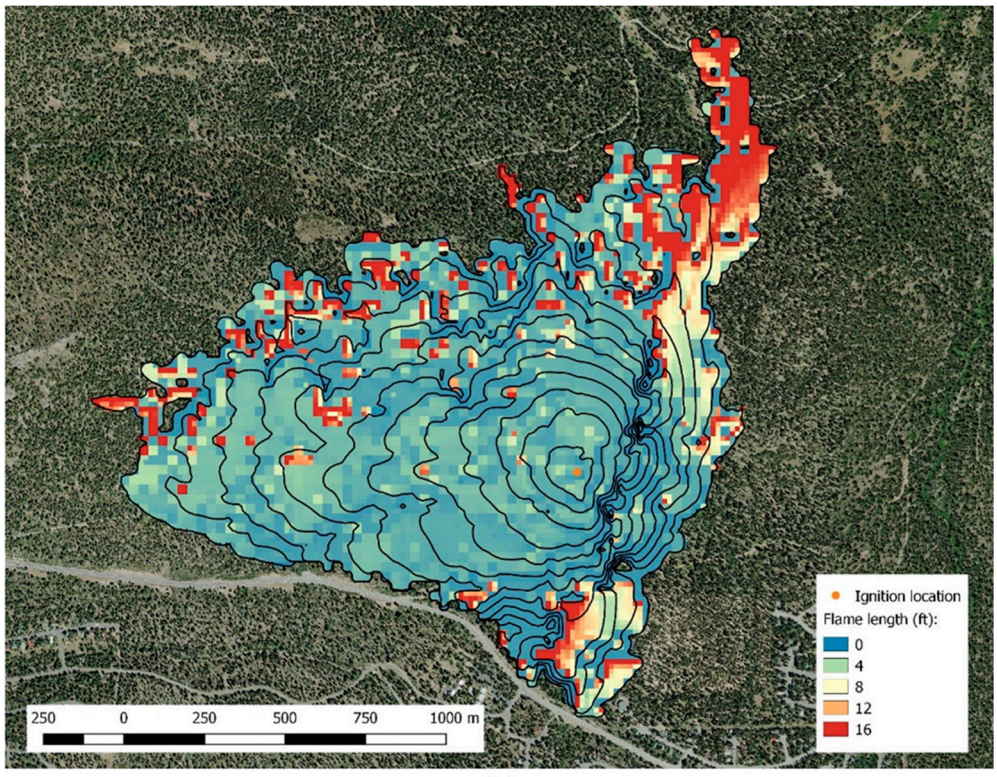

(b)

Figure 9. Example ELMFIRE fire spread simulation for individual fire ignition. (**a**) Fire type (surface fire, passive crown fire, or active crown fire). (**b**) Flame length in feet.

The primary outputs after processing are conventional annualized wildfire hazard maps at 30 m resolution within CONUS, composed of the following elements:

- Burn probability—an estimate of the likelihood that a region on the landscape burns in any single year during the simulation period.
- Fire intensity—the distribution of conditional (i.e., upon burning) flame lengths for each pixel, within discrete flame length bins.
- Exposure to embers—similar to fire intensity, a distribution of ember exposure per pixel to characterize the relative intensity of ember exposure from all modeled fires.

5.2. Validation

To validate the results from the fire behavior model, we compared the model fires against historical fires' intensity and size in aggregate. Example results from a tile-by-tile comparison of modeled and historical fires are generated as each geographic tile is run, as shown below. The modeled fire sizes are larger than in the FOD because (a) there is no fire suppression element applied within ELMFIRE, and the (b) simulation end time was randomized. To partially compensate for these limitations, as stated previously, the ignition layer was limited to sources of historical fires that were a minimum of 100 acres. This assumes that suppression measures would be effective in keeping such fires small, and of short duration. The resulting comparison of the modeled fires' sizes and intensities (Figure 10) shows that the modeled fires without explicit suppression and with randomized durations up to 7 days are systematically larger than the observed wildfires. The area of non-zero burn probabilities in the resulting hazard layers should, therefore, be considered an overestimate of the likely range of wildfire spread, which creates distributions that err on the side of caution when understanding wildfire exposure (i.e., there are likely fewer false negatives). The introduction of active fire suppression within the model is the subject of further research and may be incorporated into future versions.

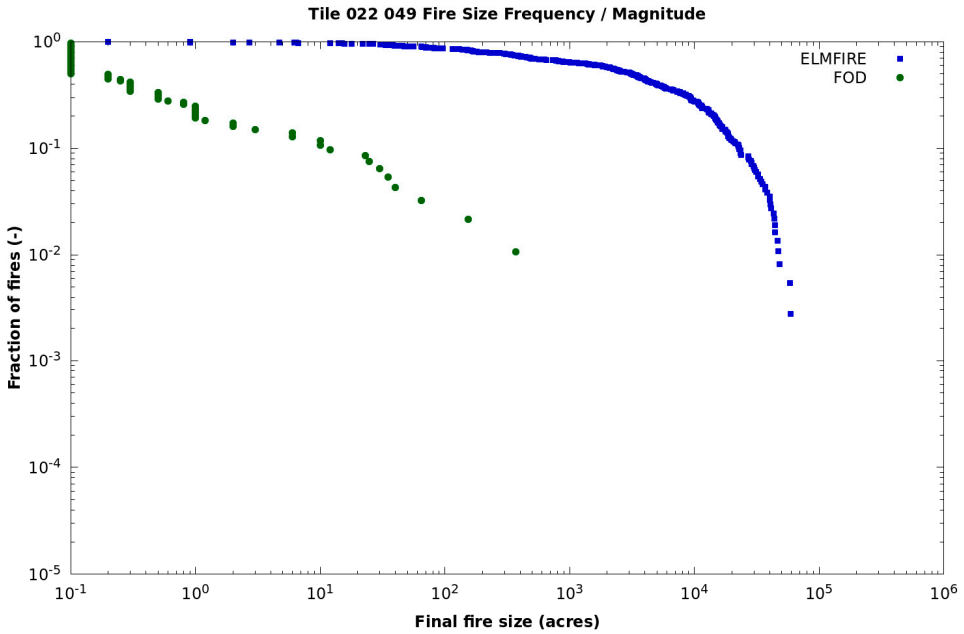

Figure 10. Historical and modeled fire sizes (in acres) versus intensity (flame length in ft).

6. Results

The construction of a national-scale, property-specific wildfire hazard model using an open-source fire behavior model, driven by openly available inputs, has been proven possible by our development of the FSF-WFM. The ability to extend the wildfire hazard into the WUI by replacing nonburnable LANDFIRE fuel designations with estimates derived from historical fire behavior in WUI areas was also shown to be feasible. Using the model in a Monte Carlo simulation, driven by historical ignition locations across CONUS to provide 30 m-resolution hazards, it was shown to be practical using commodity-scale computing

hardware. This same scheme was shown to be applicable to both current (2022) and future (2052) scenarios, given the future estimates of climate-adjusted weather conditions.

The results of the FSF-WFM model implementation are freely and publicly available through riskfactor.com, (accessed on 8 August 2022) and show property-by-property assessments of exposure to wildfire hazard. Figure 11 shows a representative parcel from the over 143 million available, and shows the levels of resolution and discrimination among properties that are available. These results are summarized at the state level in Tables 3 and 4, and Figure 12A,B, which will be discussed in more detail below.

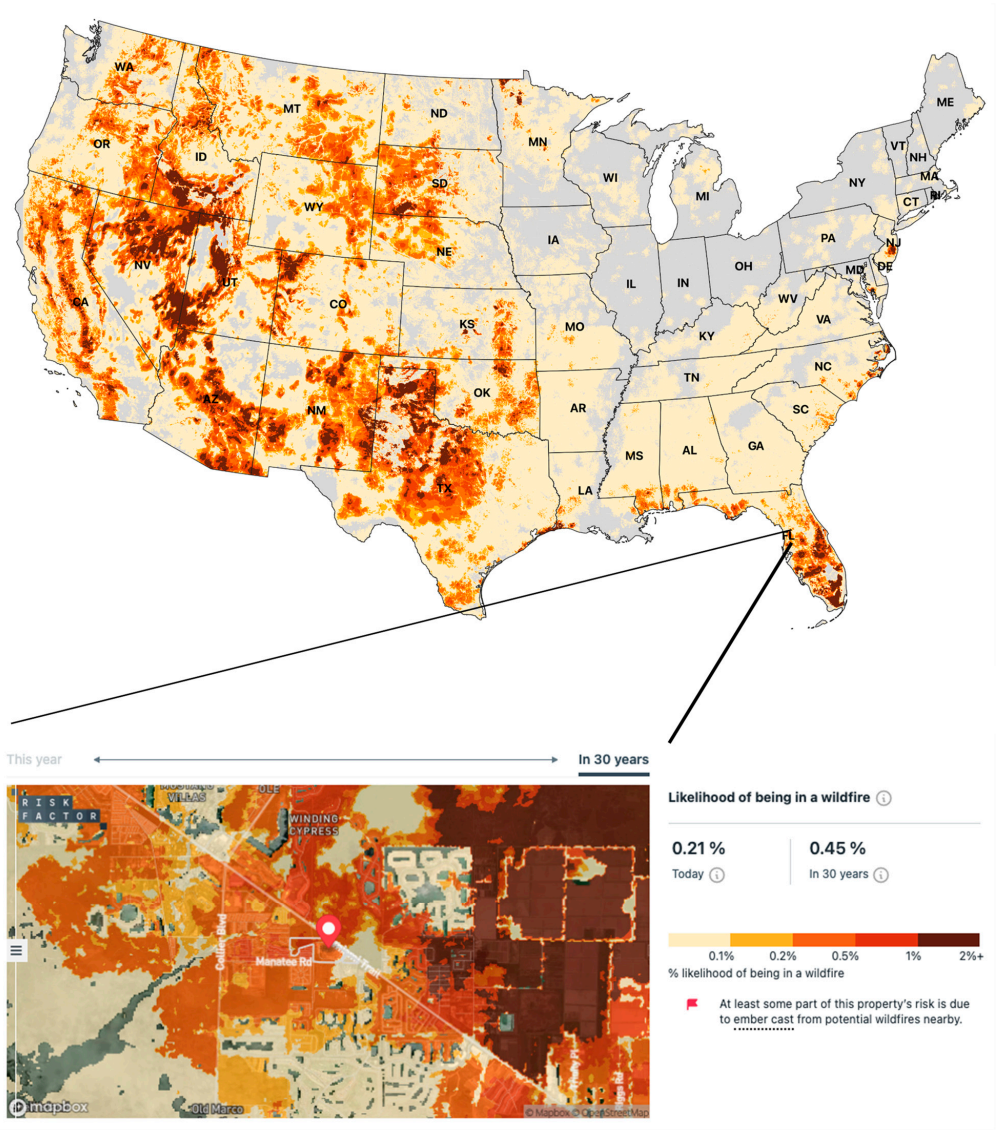

Figure 11. From riskfactor.com, (accessed on 8 August 2022): (bottom) a representative description of property-level exposure (in Naples, FL), showing the high-resolution, property-specific nature of the estimates that are produced by the FSF-WFM. Colors depict the probability (%) at 30 m resolution of being impacted by wildfire hazard during the year 2022. The likelihood numbers at right are estimates of annual likelihood of wildfire for the property at the red pin (center), and which is predicted to more than double by 2052. (Top) CONUS burn probability at 30 m resolution for 2022; gray areas show areas with negligible exposure.

Table 3. Top 25 state ranking by "any risk" (cumulative burn probability of >1%).

State	Total Properties	Any Risk	Pct Any Risk
Texas	11,957,707	9,450,091	79.03
Florida	8,975,280	7,197,685	80.19
California	11,341,383	7,131,849	62.88
North Carolina	5,451,278	3,126,130	57.35
Alabama	3,019,300	2,727,455	90.33
Georgia	4,413,839	2,482,091	56.23
Arizona	3,225,763	2,463,019	76.35
Virginia	3,795,418	2,265,927	59.70
South Carolina	2,616,091	2,068,048	79.05
Colorado	2,491,610	2,000,321	80.28
Oklahoma	2,215,755	1,901,850	85.83
Tennessee	3,278,739	1,879,316	57.32
New Jersey	3,449,541	1,859,395	53.90
Mississippi	1,904,494	1,695,462	89.02
Arkansas	1,923,556	1,558,005	81.00
Missouri	3,191,502	1,503,143	47.10
Minnesota	2,964,708	1,472,206	49.66
New Mexico	1,495,392	1,380,736	92.33
Louisiana	2,365,207	1,254,936	53.06
Utah	1,363,463	1,153,356	84.59
Kansas	1,633,521	1,087,988	66.60
New York	5,376,613	999,217	18.58
Washington	3,031,769	996,960	32.88
Oregon	1,807,336	911,745	50.45
Idaho	1,036,925	878,068	84.68

Table 4. Top 25 state ranking by "major risk" (cumulative burn probability of >3%).

State	Total Properties	Major Risk	Pct Major Risk
California	11,341,383	2,554,777	22.53
Texas	11,957,707	1,686,571	14.10
Florida	8,975,280	1,540,413	17.16
Arizona	3,225,763	998,241	30.95
Oklahoma	2,215,755	451,928	20.40
Utah	1,363,463	425,163	31.18
New Mexico	1,495,392	409,538	27.39
Nevada	1,209,308	314,203	25.98
Idaho	1,036,925	196,014	18.90
Washington	3,031,769	187,275	6.18
Colorado	2,491,610	177,081	7.11
New Jersey	3,449,541	171,568	4.97
Montana	894,052	167,040	18.68
South Dakota	666,388	164,702	24.72
Mississippi	1,904,494	121,367	6.37
Wyoming	339,209	113,570	33.48
North Carolina	5,451,278	96,774	1.78
Kansas	1,633,521	81,309	4.98
Oregon	1,807,336	70,680	3.91
Alabama	3,019,300	53,726	1.78
Nebraska	1,138,191	50,150	4.41
South Carolina	2,616,091	46,292	1.77
North Dakota	679,023	33,737	4.97
Louisiana	2,365,207	23,783	1.01
Minnesota	2,964,708	19,929	0.67

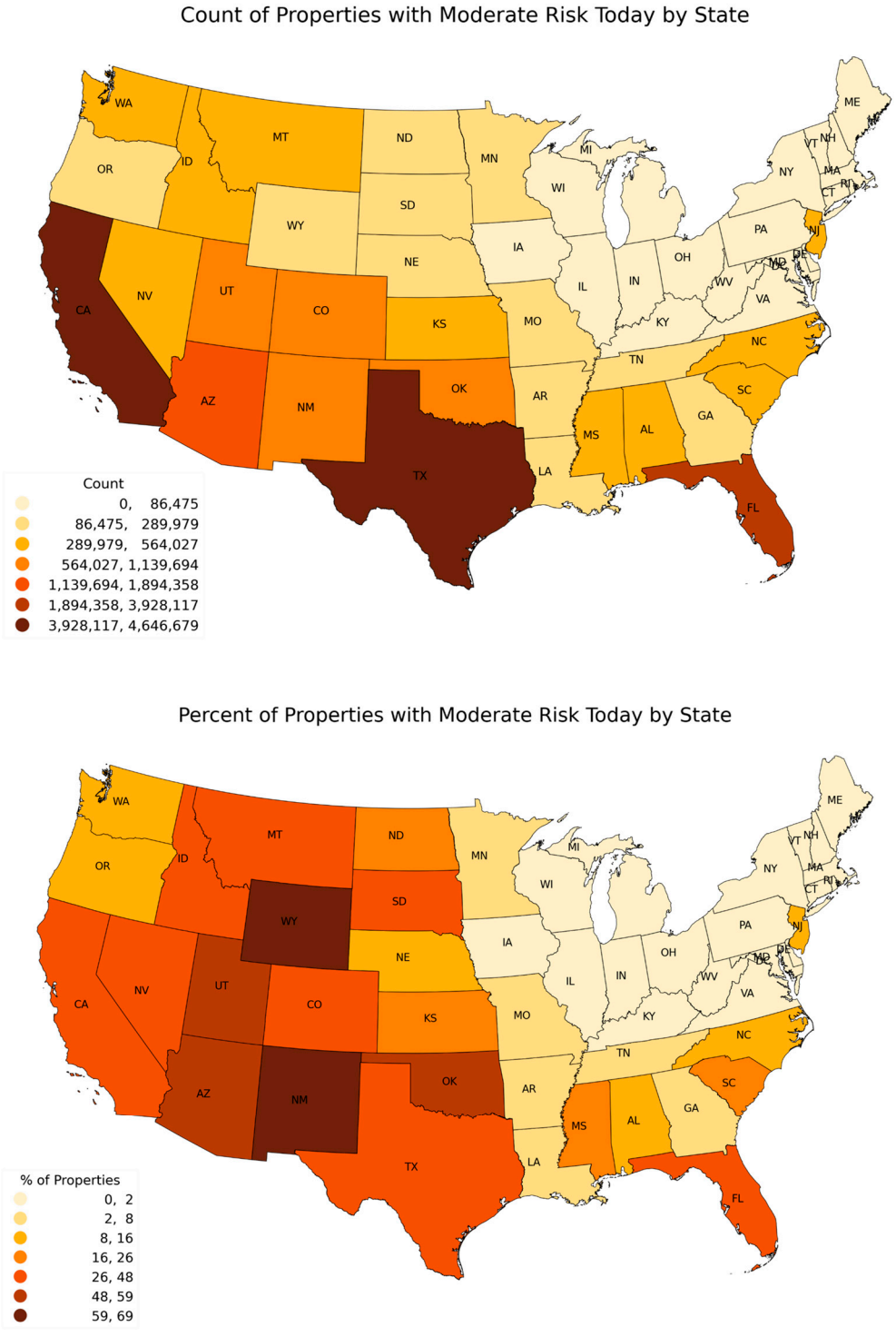

(**A**)

Figure 12. *Cont*.

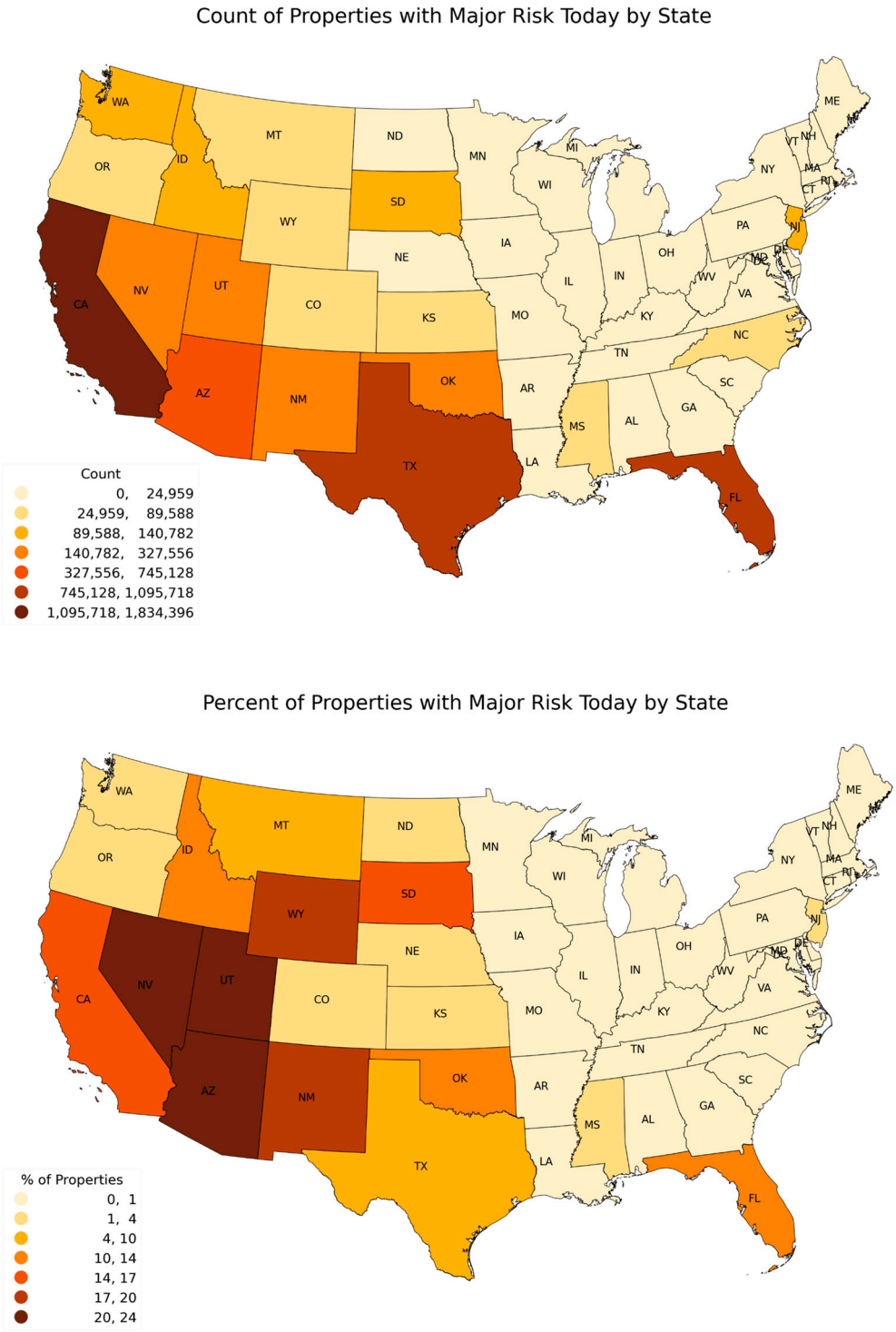

Figure 12. (**A**) Geographic distribution of "any exposure" to wildfire (>1% cumulative exposure): those individual properties with >1% cumulative exposure over 2022–2052 were counted on a state by state basis, and compared to the total number of all properties. (**B**). Geographic distribution of "major exposure" to wildfire (>3% cumulative exposure): those individual properties with >3% cumulative exposure over 2022–2052 were counted on a state by state basis, and compared to the total number of all properties.

The spatial variability in the distributions of the hazard at 30 m resolution, including within the WUI and the prevalence of hazard in the Eastern as well the Western U.S., highlight the importance of understanding wildfire risk at a property level across CONUS. While this paper focuses on the methodology and defers a thorough analysis of results to a later study, we present some general results to provide the reader with a sense of feasibility of the FSF-WFM to address current and future wildfire exposure. Overall, the results estimate that 71.8 million properties have a burn probability of >0 in the current environment (2022) and that probability increases by 11% over the next 30 years, and grows to 79.8 million properties in CONUS in 2052. Many of those properties have low, but not zero, burn probabilities from the model so we choose to describe two general levels of wildfire hazard based on a cumulative burn probability of 3% over the 30-year period, which we label "any exposure", and a cumulative likelihood of 10% over the 30-year period, which we label "major exposure". When looking at those two categories, we find about 20.2 million properties in the CONUS being subject to "any exposure" and 5.9 million properties being at "major exposure" to wildfire over the 30-year period (2022–2052). These property counts represent about 15% and 5% of all property parcels in the CONUS, which further highlights the large exposure of properties in the US to wildfire exposure. For further context, flooding, which is generally referred to as the most widespread climate peril in the US, impacts about 21.8 million properties at the "any flood" level (equivalent to 6% 30-year aggregate) and about 14.6 million properties at the "significant flood" level (equivalent to 26% 30-year aggregate) [56].

7. Any Exposure

Table 3 and Figure 12A report the results of the model when applied against individual property structures and parcel centroids (on parcels without buildings). The results indicate that the top five states in regards to "any exposure" are Texas, Florida, California, North Carolina, and Alabama. In those 5 states alone, there are nearly 30 million properties with at least a 1% cumulative probability over the next 30 years of being impacted by a wildfire. Figure 12A (upper) further illustrates that the distribution of properties "any exposure" of wildfire are disproportionately located in Texas, California, and the Southeastern US. When taking into account "any exposure" of wildfire relative to the total housing stock in Figure 12A (lower), the Mountain West states of Montana, Idaho, Wyoming, and Utah emerge as a cluster of disproportionate potential impact, along with New Mexico, Oklahoma, Mississippi, and Alabama across the southern tier of the country. The Midwest and Northeast are relatively lower in regards to "any exposure" to wildfire over the next 30 years, which is expected given the climate conditions that generally drive the peril.

7.1. Major Exposure

Table 4 and Figure 12B report the results for only those properties at "major exposure" to wildfire (3% cumulative likelihood over the 30-year period). When only looking at this subset of properties, California stands out as having the most exposure, with over 2.5 million properties in this category. Texas, Florida and Arizona, at 1.7, 1.5, and nearly 1 million properties at "major exposure", respectively, together with California, account for over 6.5 million properties that meet the threshold of having at least 3% cumulative wildfire exposure over the next 30 years. Figure 12B (upper) highlights the fact that when shifting from "any exposure" to "major exposure", the majority of that exposure is held in the Western US, with Florida, Mississippi, New Jersey, and North Carolina standing out as states in the eastern half of the country with higher levels of exposure than the surrounding areas. Figure 12B (lower) shifts that impact slightly when accounting for the exposure as a proportion of properties in the state. Using that metric, Arizona, Utah, and Wyoming carry the most exposure to wildfire hazard, followed by their western neighbors, California and Nevada.

The estimated geographic distribution of change in wildfire exposure due to climate change is shown in Figure 13. The percentage increase between the current year and

30 years into the future in the average burn probabilities of properties with at least 0.03% risk is at least 100% in many of the counties across the country. The annual burn probability of 0.03% corresponds to at least a 1% cumulative likelihood over a 30-year period. With higher burn probabilities, a higher incidence of losses is expected over time, as properties are exposed more often to wildfires.

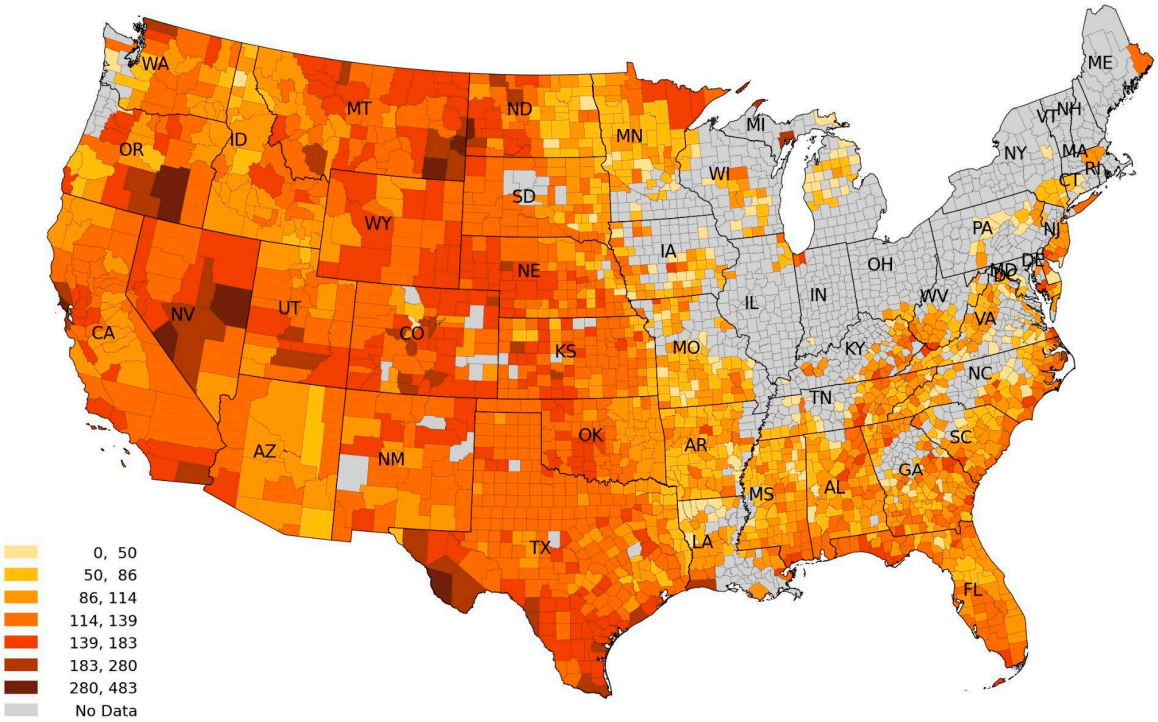

Figure 13. Percent Increase in annual likelihood of wildfire exposure among properties with at least 0.03% annual likelihood of wildfire exposure.

Finally, a fire factor risk assessment was created on a property-level basis across CONUS. Property parcel geometries are provided by the Lightbox public-record property boundaries database. Building footprint geometries are defined by Mapbox. First Street performed a geometric intersection to match parcels to building footprints. Footprints that cross parcel boundaries were subdivided, such that no footprint geometry crosses parcel boundaries. Since some parcels intersect multiple footprint geometries, the building footprint with the largest area was designated the primary footprint.

To evaluate the exposure to wildfire flames and embers, each hazard layer was queried at the geometric centroid of each building footprint and parcel. For scoring purposes, at properties with a building footprint, the statistic at the primary footprint centroid was recorded; for parcels without a building footprint, the parcel centroid was recorded. The assignment of a 30-year, climate-adjusted aggregated wildfire risk score was then computed by calculating the likelihood and nature of exposure through burn probabilities in and belongingness to an ember zone for a building or parcel as representative of the risk for each property for 2022 and then for 2052, and then linearly interpolating this across that 30-year period.

The annual risk, as defined by burn probability in and belongingness to an ember zone for each year, was summed across the 30-year period and was used to derive the total chance of exposure over that 30-year period, which includes climate change effects. The fire factor scoring rubric is included in Table 5.

Table 5. Fire factor assignment.

Fire Factor	Criteria
1	No modeled exposure of being in a wildfire (burn probability) and no modeled exposure to embers (including not being in an ember zone) are considered to have minimal risk.
2	Located in areas exposed to embers through the created ember zone or in an area with less than a 1% cumulative chance of burning over 30 years.
3	With 1–3% chance of burning over 30 years.
4	With a 4–6% chance of burning over 30 years.
5	With a 7–9% chance of burning over 30 years.
6	With a 10–14% chance of burning over 30 years.
7	With a 14–20% chance of burning over 30 years.
8	With a 21–26% chance of burning over 30 years.
9	With a 27–36% chance of burning over 30 years.
10	With more than a 36% chance of burning over 30 years.

7.2. Assumptions and Limitations

The wildfire hazard estimates from the methodology described in this research paper offer insights into the current and future wildfire exposure at 30 m resolution across CONUS, using widely accepted input layers from LANDFIRE and using the Rothermal-based ELMFIRE fire behavior model that has already undergone peer-review and validation. The resulting estimates of wildfire hazard exposure provide a first view of national level, high precision, property-level exposure estimates across the US in a framework that takes into account both current and future changing exposure to wildfire. The results identify at least some level of exposure in many places that are generally not thought of as having a wildfire problem, but they also underscore the fact that there is a tremendous amount of "major exposure" in the Western US, and specifically in the WUI areas in California and the Mountain West States. These insights are intended to complement the work carried out by the WRC program by providing a property-level equivalent to the community level tool already in the public domain, using similar but independent Rothermel-based fire behavior modeling. Nevertheless, there are a number of acknowledged limitations in our methodology, many of which have already been noted, but the implications of which are discussed in the following list:

- Lack of explicit fire suppression: since the fire behavior model ELMFIRE does not explicitly include suppression effects, the model tends to overestimate the size and intensity of wildfires, which leads to an overestimate of the extent of wildfire exposure.
- Variable length of wildfire burn time: ELMFIRE randomizes the length of the time for each modeled wildfire, leading to overestimates in the size and intensity of wildfires. The amount of time and the number of simulated fires needed to drive the Monte Carlo simulation towards stable statistics varies geographically across the model domain.
- Extremely large fires: the simulation method does not capture the behavior of extremely large fires, since the fire weather forcing the simulation is not coupled with the fire behavior model.
- House to house ignition: while the replacement of the non-burnable fuels in the LANDFIRE representation of the WUI with estimates of burnable fuels allows wildfires to propagate through the WUI more accurately, the ignition and subsequent contribution to wildfire by the buildings/houses themselves to the hazard within the WUI is not yet included in FSF-WFM.
- Vegetation changes: the vegetation between 2022 and 2052 was held constant, although it is anticipated that changes in vegetation composition and density, and thus fuels, will be driven to some degree by climate change. Keeping the 2022 fuels constant for the assessment of 2052 future exposure underestimated the total possible changes due to the climate, but focuses attention on the direct effects of the climate and future

weather on the state of those fuels, which has significant implications for wildfire ignitions, intensity, and spread.

- Future weather approximation: A comprehensive sensitivity analysis to the bias-adjustment techniques used for climate adjustment is warranted. In addition, the high quality of the winds in the 2048–2057 simulations (the same as the 2011–2022 observations) is an advantage over using modeled winds, but is nevertheless an assumption. Most importantly, since the length and severity of droughts captured in the 2011–2020 time series do not change for the 2048–2057 simulation, the possible impact of those droughts, as they increase in frequency and severity, is unresolved.
- Incomplete fuels/disturbances for fuel updates: disturbances are not evenly reported across the US, and some areas (e.g., private lands in the Eastern US) are not well known.
- Ignition locations: using only historical fire ignition locations limits the possible impact of climate change on plausible fire locations, and the omission of random lightning strikes leaves some areas under-sampled. Additionally, a nuance of the decision to build the ignition density surface from only >100 acre fire occurrence data is that ignition density will be zero in areas that have not experienced fires >100 acres, even if those areas have experienced fires <100 acres. Dillon et al. [39] noted that in areas where management strategies have previously been successful at limiting large fire occurrence, burn probability modeling based only on large fire occurrence may underestimate burn probability. For that reason, Dillon et al. [39] developed an ignition density surface weighted as 98% large fire occurrence and 2% small fire occurrence, and such an approach could likely be used in future work.
- No future land use changes: to focus on the impacts of climate change on the existing parcels under future wildfire exposure, we have elected to keep the built environment constant, and to assume no changes in land use or condition. This simplifying assumption is useful for its stated purpose, but we also recognize that changes in land use will also precipitate changes in likely future ignition locations, WUI locations, fuel conditions and types.

8. Discussion and Concluding Points

The methodology presented computes the physical hazard associated with wildfire incidence for the contiguous United States at 30 m resolution, and is expressed through hazards quantifying burn probability, flame length, and ember spread for the years 2022 and 2052, based on 10-year representative Monte Carlo simulations of wildfire behavior. This methodology uses updated fuels estimates that integrate known disturbances, current and estimated future weather characteristics that are useful for understanding aggregate wildfire exposure at a high resolution, and uses a model of wildfire behavior that integrates ignition, time of burn, and spread. This work does not develop new techniques or approaches to fire probability and hazard modeling, but rather integrates several existing methods and implements a computationally efficient and scalable modeling techniques to allow for new high-resolution, CONUS-wide hazard generation—all based on existing data, fire science, and hazard modeling paradigms developed by others in the wildfire science community. We have extended these approaches to estimate not only updated, current wildfire hazards but also extending those to estimate climate change's future impacts on these hazards.

The methodology for the augmentation of the US Forest Service's LANDFIRE-based estimates of fuel types, densities, and conditions at a 30 m resolution is presented using an open-source, Rothermel-based wildfire behavior model, ELMFIRE, for computation. The replacement of non-burnable fuel types in LANDFIRE that represent the built environment within the wildland–urban interface (WUI), with fuel inputs from the results of machine-learning estimates trained on data from historical fires, allow the propagation of wildfire through the WUI in a way that more closely resembles the observed conditions, and often results in non-zero burn probabilities for these areas. This serves as a notable improvement and opportunity for future fire models to replicate such an approach to improve their

modeling. The wildfire hazard derivation overall is heavily dependent upon the updated LANDFIRE 2016 fuel layers, and significant effort was undertaken to assemble all known disturbances throughout 2020. Combined, this provides a repeatable methodology for future research looking to incorporate current fuel estimates, when annually updated LANDFIRE data are not available.

Other inputs required for ELMFIRE include topography from the USGS National Elevation Database, and weather (winds, air temperatures, humidity, and precipitation), for which the 2011–2020 NOAA RTMA hourly time series was selected. This 10-year time series provided an adequate range of possible weather conditions for the Monte Carlo simulation, where ELMFIRE was run approximately 100 million times to produce an estimate of the 2022 wildfire hazards for CONUS. To enable an estimate of the future hazard, this same hourly time series was bias-adjusted using MACAv2 daily downscaled IPCC CMIP5 RCP4.5 climate model ensemble results. Since accurate winds are crucial to the accurate prediction of wildfire behavior, and winds have a direct and significant influence on ELMFIRE results, we elected to hold winds constant between the 2022 and 2052 simulations, and bias-adjust only air temperature, humidity, and precipitation. This choice reduced the uncertainties introduced into the hazards from the fire behavior model, and instead focuses on the impact of climate change on the condition of the fuels for the 2048–2057 Monte Carlo simulations. Vegetation was likewise held constant between the 2022 and 2052 Monte Carlo simulations, as a reasonable but conservative approximation over 30 years' time. The differences in wildfire hazards in the 2052 estimates are then based solely upon climate's impact on the state of the fuels and generally hotter, drier conditions are thought to influence greater burn probabilities in the 2052 estimates. Due to the vegetation being held constant, these 2052 estimates should be considered conservative estimates of future wildfire exposure.

Fire ignition locations for the simulations were kept the same for 2011–2020, as for the 2048–2057 Monte Carlo simulations, and were created from the historical origins of significant fires greater than 100 acres. This lower limit on fire size was used to implicitly account for fire suppression activities that are not currently modeled in ELMFIRE. Over 100 million fires were modeled for each simulation period, and 8–10% of those model fires grew and were tracked at 30 m resolution across the landscape for up to 7 days apiece. Outputs were aggregated to create burn probability, flame length, and ember spread hazard estimates at 30 m horizontal resolution for CONUS. These hazard estimates are conducive to the assessment of the exposure of US properties to wildfire flames and/or embers. Comparisons with historical wildfire intensities and sizes show that the lack of explicit fire suppression effects in the FSF-WFM produces overestimates of fire sizes and intensities, so the resulting wildfire hazards should be considered to be conservative overestimates. Comparisons to historical wildfire losses and the US Forest Service's WFC products generally show consistency at the state and community levels, but additional validation using historical losses at the building level should be undertaken in the future. The FSF-WFM wildfire hazards will produce fewer false negatives of risk assessments at the property level, and when combined with specific building vulnerability, could be used to provide similarly conservative estimates of climate-adjusted wildfire losses at the building level.

Wildfire hazards are estimated to be non-zero for 71.8 million of the over 140 million properties in CONUS, and will include an additional 11% properties over the next 30 years, due to climate change impacts on fuel conditions. While most of the overall wildfire risk is associated with properties west of 100 degrees W longitude in the American West, much of the change in wildfire exposure is observed east of the Mississippi River in areas not normally associated with large wildfire exposure. Over 5.9 million properties are found to have a "major" aggregate wildfire exposure of 10% over the 30-year analysis period from 2022–2052, which invites further investigation at the hyper-local level to discover ways to mitigate that exposure. Since the fuels and winds have been held the same between 2022 and 2052 in our simulations, the implication is that any increase in wildfire exposure is

due to the future weather's increased impacts on fuel conditions. Thus the influence of climate change on fuel conditions is the primary cause of the estimated increase in wildfire exposure throughout the country.

The FSF-WFM represents the first national-scale, property-level wildfire exposure model that has been developed using a geographically-consistent approach. The ability to consistently assess wildfire exposure, and thus risk for every property across the CONUS, should give local, state, and national government decision makers another data tool to help guide the allocation of resources, allow property owners to better assess their risk and implement meaningful solutions to reduce that risk, and provide financial markets with the opportunity to price risk into the cost of property more effectively through insurance, mortgage, and other financial products.

Author Contributions: Conceptualization, E.J.K. and D.S.; methodology, D.S., M.A., J.R.P., C.L., C.R.L., K.D.W., G.W.J. and O.M.D.; software, C.L., K.D.W., B.M., G.W.J., K.M.; validation, G.W.J., C.R., K.M., A.M., H.H. and M.B.; formal analysis, C.L., C.R.L., M.A.; investigation, B.W., J.R.P., B.M., M.B., K.L., H.H., A.M., F.C.; resources, J.R.P., M.A., O.M.D.; data curation, N.F., C.R., C.R.L.; writing—original draft preparation, E.S., J.R.P., E.J.K., C.R.L. and C.L.; writing—review and editing, E.S.; visualization, C.R.L., C.L., M.A., N.F. and J.R.P.; supervision, D.S.; project administration, E.J.K., M.A. and D.S.; funding acquisition, E.J.K. All authors have read and agreed to the published version of the manuscript.

Funding: This research received no external funding, and was entirely supported by the philanthropic donors to the First Street Foundation. Cloud compute credits in support of this research were graciously provided through Amazon Web Services by the Amazon Sustainability Data Initiative (ASDI).

Institutional Review Board Statement: Not applicable.

Informed Consent Statement: Not applicable.

Data Availability Statement: The resulting FSF-WFM hazard layers and associated property-specific vulnerability and economic assessments will be freely and publicly available for noncommercial use at https://riskfactor.com, (accessed on 8 August 2022). The public availability of this climate information is meant to inform the public, enable new research efforts on wildfire risk, level the playing field with private commercial interests that already have access to this kind of information, and help address the privatization of climate impact information.

Acknowledgments: The authors are grateful for the philanthropic support provided to the First Street Foundation to enable this research. We are also thankful for the helpful comments from three anonymous reviewers of this manuscript. The First Street Foundation Wildfire Model is the product of a collaborative partnership between the First Street Foundation and the Pyregence Consortium, which includes the Spatial Informatics Group (SIG), Reax Engineering, and Eagle Rock Analytics. The Pyregence Consortium is grateful for the California Energy Commission's support [EPC-18-026] of the Consortium that paved the way for this new study. The authors thank Jeff Knickerbocker (SIG) for his compute and hardware support, and Teal Dimitrie, Jean-Pierre Wack and Alecio O'Day for their project management of the Pyrgence Consortium's efforts. Special gratitude is extended to the following individuals who provided valuable insights related to the FSF-WFM and its inputs: Janice Cohen of the National Center for Atmospheric Research; LeRoy Westerling and John Abatzoglou of the University of California Merced; Mark Finney, Gregory Dillion, Karen Short, and Eva Karau of the Rocky Mountain Research Station; Joel Reynolds, Marybeth Keifer, and Windy Bunn of the National Park Service; Ben Sleeter and Nathan Wood from the U.S. Geological Survey; Joshua Picotte, Tobin Smail, and Inga La Puma of the LANDFIRE team. The authors are grateful to Ana Pinheiro-Privette from the Amazon Sustainability Data Initiative for her support of their compute and data services workloads on AWS.

Conflicts of Interest: The authors declare no conflict of interest.

Appendix A. Data Sources Used in the Development of the FSF-WFM

Name	Subject	Source
LANDFIRE	Fuels	LandFire.gov (accessed on 1 June 2022)
USGS NED	Topography	https://www.usgs.gov/programs/national-geospatial-program/national-map (accessed on 1 June 2022)
USDA Forest Service's Fire Occurrence Database (FOD)	Ignition Locations	https://doi.org/10.2737/RDS-2013-0009.5 (accessed on 1 June 2022)
MTBS, NIFC	Historical fires	https://www.mtbs.gov and https://www.nifc.gov (accessed on 1 June 2022)
NOAA RTMA	Weather, 2011–2020	https://mtarchive.geol.iastate.edu/ and https://www.ncei.noaa.gov/has/HAS.FileAppRouter?datasetname=9950_01&subqueryby=STATION&applname=&outdest=FILE (accessed on 1 June 2022)
MACAv2	Climate	MACA data portal (accessed on 1 June 2022)
Future 2052 Weather	Weather estimates for 2048-2057; Derived from MACAv2 and NOAA RTMA time series	derived
Future 2052 Fuels	Assumed to be same as 2022 for V1	Held constant
Property Boundaries	Lightbox	commercial
Building Footprints	Mapbox	commercial
Building Density	Derived from Building footprint information	derived

Appendix B. Treatment Disturbance Inputs

Dataset Name	Source Data Link
Hazardous Fuels Treatments—Fire—USFS	https://apps.fs.usda.gov/arcx/rest/services/EDW/EDW_HazardousFuelsTreatments_01/MapServer/3 (accessed on 1 June 2022)
Hazardous Fuels Treatments—Other—USFS	https://apps.fs.usda.gov/arcx/rest/services/EDW/EDW_HazardousFuelsTreatments_01/MapServer/4 (accessed on 1 June 2022)
Hazardous Fuels Treatments—Mechanical—USFS	https://apps.fs.usda.gov/arcx/rest/services/EDW/EDW_HazardousFuelsTreatments_01/MapServer/5 (accessed on 1 June 2022)
Hazardous Fuels Treatments—All Other Values—USFS	https://apps.fs.usda.gov/arcx/rest/services/EDW/EDW_HazardousFuelsTreatments_01/MapServer/7 (accessed on 1 June 2022)
Timber Harvest—USFS	https://apps.fs.usda.gov/arcx/rest/services/EDW/EDW_TimberHarvest_01/MapServer/8 (accessed on 1 June 2022)
CALMAPPER Treatment Projects	https://egis.fire.ca.gov/arcgis/rest/services/CalMapper/CalMAPPER_Public/FeatureServer/2 (accessed on 1 June 2022)
CALFIRE Priority Treatment Projects	https://services1.arcgis.com/jUJYIo9tSA7EHvfZ/ArcGIS/rest/services/PriorityProjects2019/FeatureServer/0 (accessed on 1 June 2022)
CALFIRE Timber Harvest	https://services1.arcgis.com/jUJYIo9tSA7EHvfZ/ArcGIS/rest/services/CAL_FIRE_Timber_Harvesting_Plans_All_WGS84/FeatureServer/0 (accessed on 1 June 2022)

Dataset Name	Source Data Link
CALFIRE Fire Perimeters—Prescribed Fire	https://egis.fire.ca.gov/arcgis/rest/services/FRAP/FirePerimeters_FS/FeatureServer/1 (accessed on 1 June 2022)
CALFIRE Forest Health CCI Awarded Projects 2017-18	https://services1.arcgis.com/jUJYIo9tSA7EHvfZ/ArcGIS/rest/services/Forest_Health_CCI_Awards_2017_2018/FeatureServer/0 (accessed on 1 June 2022)
Treatment areas—National Park Service	https://mapservices.nps.gov/arcgis/rest/services/WildlandFire/WildlandFire/FeatureServer/5 (accessed on 1 June 2022)
Treatment areas—ID—BLM	https://navigator.blm.gov/api/share/e5fb96b234d32c5a (accessed on 1 June 2022)
Treatment areas & Harvest—OR Dept Forestry	https://gisapps.odf.oregon.gov/data/FernsNoapsPolygons.Zip (accessed on 1 June 2022)
Treatment areas—CA—BLM	https://navigator.blm.gov/api/share/a446b6874c2a37fc (accessed on 1 June 2022)
Treatment areas—NM—BLM	https://gis.blm.gov/nmarcgis/rest/services/Range/BLM_NM_Vegetation_Treatments/MapServer/0 (accessed on 1 June 2022)
Harvest—WA Dept Natural Resources	https://gis.dnr.wa.gov/site2/rest/services/Public_Forest_Practices/WADNR_PUBLIC_FP_FPA/MapServer/6/ (accessed on 1 June 2022)

Appendix C. Fires Used to Estimate Fuels in WUI Areas

Incident Name	State	Ignition Date	Lat.	Long.	Acres Burned	Total Structures Damaged	Total Structures Destroyed	Total Structures Threatened
Shockey	CA	9/23/2012	32.618	−116.335	2667	10	45	125
Bastrop County Complex	TX	9/4/2011	30.13	−97.235	31,838	0	1709	1160
Pine Creek	OR	7/14/2014	44.808	−120.273	31,033	0	0	16
Highway 613 Fire	MS	10/31/2014	30.507	−88.526	635	0	0	30
Carlton Complex	WA	7/14/2014	48.248	−119.96	276,091	0	471	1103
Mills Canyon	WA	7/8/2014	47.626	−120.297	21,952	0	3	571
Anaconda	UT	7/20/2014	40.562	−112.237	1142	0	0	30
High Range	ID	8/3/2014	45.743	−116.493	5328	0	3	30
Happy Camp Complex	CA	8/14/2014	41.707	−123.196	118,491	2	6	767
Knf Beaver	CA	7/30/2014	41.89	−122.871	34,274	0	6	235
Snag Canyon	WA	8/3/2014	47.167	−120.475	12,508	1	22	279
Johnson Bar	ID	8/3/2014	46.096	−115.614	15,170	0	0	57
Rain	ID	8/3/2014	45.583	−115.185	4772	0	0	4
Assayii Lake	NM	6/13/2014	36.032	−108.844	13,176	0	5	50
Slide	AZ	5/20/2014	35.009	−111.802	22,698	0	0	350
French	CA	7/28/2014	37.294	−119.36	14,534	0	0	106
Way	CA	8/18/2014	35.735	−118.461	3947	12	12	1500
Eiler	CA	7/31/2014	40.799	−121.558	30,967	0	30	755
Taylor Mountain Road	UT	7/5/2014	40.531	−109.573	2965	3	3	50
Triple G	FL	5/9/2015	26.118	−81.591	736	0	0	0
Grand Lake	FL	4/19/2015	25.75	−80.455	1368	0	0	11
Lime Hill	OR	8/5/2015	44.37	−117.33	12,210	0	5	4
Dry Gulch	OR	9/12/2015	44.829	−117.139	18,369	0	0	507
Mann	ID	8/18/2015	44.263	−116.84	1527	0	0	30
Mm43 Hwy 52	ID	6/25/2015	43.977	−116.4	11,022	2	0	10
Celebration	ID	6/6/2015	43.26	−116.497	7281	0	0	0
Soda	ID	8/10/2015	43.319	−116.861	282,888	1	1	145
Sleepy Hollow	WA	6/28/2015	47.455	−120.375	3238	27	35	0
I-90	WA	7/19/2015	47.013	−119.959	1397	0	0	20
Highway 8	WA	8/4/2015	45.802	−120.184	35,296	0	0	350

Incident Name	State	Ignition Date	Lat.	Long.	Acres Burned	Total Structures Damaged	Total Structures Destroyed	Total Structures Threatened
Brown Ranch	TX	8/11/2015	29.993	−100.428	17,881	0	3	22
County Line 2	OR	8/12/2015	44.829	−121.412	68,189	0	7	1452
Roosa Gap	NY	5/3/2015	41.638	−74.421	2747	0	0	11
Pipeline 1	PA	5/3/2015	41.123	−75.677	666	0	0	0
North	CA	7/17/2015	34.372	−117.474	4366	5	23	700
Gilmore Gulch	WA	7/5/2015	46.16	−116.964	8074	0	0	11
Tucannon	WA	8/29/2015	46.359	−117.678	2809	0	0	140
Ridge Road	ND	4/14/2015	48.079	−103.09	3390	0	0	0
Powerline	OK	1/26/2015	35.364	−95.884	1183	0	0	11
Highway	CA	4/19/2015	33.907	−117.624	1212	0	0	252
Z Bar 7	OK	3/31/2015	36.664	−96.149	5908	0	0	0
2230 Road	OK	4/4/2015	36.454	−96.158	2650	0	6	0
Wf West End 2015	TX	2/13/2015	29.588	−94.341	6590	0	0	0
Razor Fire	PA	4/18/2015	40.779	−75.682	728	0	0	4
Boars Hammock	FL	4/26/2015	26.885	−81.253	790	0	0	0
Tallgrass East	KS	4/14/2015	38.41	−96.525	1745	0	0	0
Wf Texas Point Northeast	TX	10/4/2015	29.705	−93.93	4635	0	0	0
Greenwood	OK	3/23/2015	36.054	−96.319	5774	0	0	0
West Prong	OK	3/24/2015	36.413	−96.064	3676	0	1	500
Trail 12	FL	5/5/2015	28.788	−82.366	1041	0	0	0
Station	WY	10/11/2015	42.882	−106.18	9845	94	46	392
Big Spring Branch	WV	11/17/2015	37.701	−81.825	1044	0	0	0
Little Horse Creek	WV	11/17/2015	38.132	−81.851	1145	0	0	0
Little Jerrell	WV	11/18/2015	37.985	−81.646	1193	0	0	0
Trace Fork	WV	11/14/2015	37.434	−81.934	784	0	0	0
Kearny River	AZ	6/17/2015	33.068	−110.92	1543	5	5	50
Willow	AZ	8/8/2015	34.837	−114.544	6084	40	31	710
Goodell	WA	8/11/2015	48.683	−121.227	6624	0	0	50
Stouts Creek	OR	7/30/2015	42.859	−122.985	27,570	0	0	645
Route Complex	CA	7/31/2015	40.601	−123.541	35,444	0	2	475
Grenade	CA	4/29/2015	33.404	−117.514	1776	0	0	0
River Complex	CA	7/31/2015	40.914	−123.364	78,531	0	0	506
Solimar	CA	12/26/2015	34.303	−119.342	1083	0	0	103
Cuesta	CA	8/17/2015	35.356	−120.612	2415	0	1	339
Parkhill	CA	6/20/2015	35.367	−120.424	1795	5	18	100
Tassajara	CA	9/19/2015	36.391	−121.589	1085	1	21	0
Lowell	CA	7/25/2015	39.212	−120.869	2633	1	3	1800
Tesla	CA	8/19/2015	37.636	−121.594	2508	0	1	0
Lumpkin	CA	9/11/2015	39.527	−121.327	1137	0	0	200
Wragg	CA	7/22/2015	38.481	−122.069	8455	5	2	700
Rocky	CA	7/29/2015	38.91	−122.45	96,125	8	96	6959
Valley	CA	9/12/2015	38.788	−122.613	77,507	95	2019	9150
Rough	CA	7/31/2015	36.852	−118.884	146,369	0	4	1536
Washington	CA	6/19/2015	38.642	−119.699	18,485	0	2	251
Butte	CA	9/9/2015	38.266	−120.592	72,894	48	901	6400
Corrine	CA	6/19/2015	37.179	−119.5	1064	0	3	250
Willow	CA	7/25/2015	37.282	−119.479	5990	0	0	455
Cape Horn	ID	7/5/2015	47.998	−116.521	1505	1	14	309
Slide	ID	8/14/2015	46.096	−115.382	13,509	0	0	29
I-90 Sprague	WA	8/1/2015	47.314	−117.934	1771	0	0	2
Carpenter Rd.	WA	8/15/2015	48.05	−118.091	62,488	0	43	1005
Lawyer 2	ID	8/11/2015	46.23	−116.108	11,378	0	0	25
Municipal	ID	8/15/2015	46.469	−116.19	1969	5	11	302
Woodrat	ID	8/11/2015	46.167	−115.771	6513	0	0	81
Tepee Springs	ID	8/12/2015	45.318	−116.116	94,878	0	6	1410
Eagle	OR	8/11/2015	45.028	−117.373	14,502	0	1	52
Canyon Creek Complex	OR	8/12/2015	44.301	−118.85	109,786	100	54	722
Black Canyon	WA	8/14/2015	47.976	−120.053	61,379	0	0	0
First Creek	WA	8/14/2015	47.929	−120.244	7971	22	19	556
Chelan Complex	WA	8/14/2015	47.912	−119.846	21,774	1	55	2948
West Fork Fish Creek	MT	8/14/2015	46.909	−114.804	14,495	0	5	372
North Star	WA	8/13/2015	48.415	−118.94	218,547	0	1	4225
Marble Valley	WA	8/14/2015	48.404	−117.892	3431	22	41	326
Renner	WA	8/14/2015	48.758	−118.193	13,975	0	0	120

Incident Name	State	Ignition Date	Lat.	Long.	Acres Burned	Total Structures Damaged	Total Structures Destroyed	Total Structures Threatened
Blue Creek	WA	7/20/2015	46.037	−118.08	5990	0	12	250
9 Mile	WA	8/13/2015	48.971	−119.296	5052	0	10	80
Limebelt	WA	8/14/2015	48.507	−119.694	137,098	0	0	20
Hidden Pines	TX	10/13/2015	30.081	−97.183	3807	2	141	406
Tunk Block	WA	8/14/2015	48.478	−119.339	180,111	0	145	3000
Liberty Hill	LA	10/13/2015	32.345	−92.907	711	0	3	12
Lake	CA	6/17/2015	34.147	−116.762	30,421	0	4	7390
Sunland	WA	5/29/2016	47.045	−119.99	1940	0	0	20
16 Mile	PA	4/20/2016	41.199	−75.149	7896	9	11	287
Bear Town	PA	4/20/2016	41.181	−75.222	649	0	0	0
Sams Point Fire-Verkeerder Fire	NY	4/23/2016	41.681	−74.343	1929	0	0	7
Road 10	WA	8/2/2016	47.23	−119.357	2750	0	8	87
Elmer City	WA	9/11/2016	47.978	−118.942	5619	0	1	140
Rocky Mtn Fire 2016	VA	4/16/2016	38.31	−78.665	9299	0	0	337
Fifteen Mile	OR	7/1/2016	45.638	−121.006	4044	0	0	45
Range 12	WA	7/30/2016	46.495	−119.869	167,604	0	0	250
County Line Road Fire	NC	3/10/2016	35.011	−79.513	1704	0	0	0
Mcbee Command	WA	7/15/2016	46.249	−119.519	1813	0	0	20
Cellar Mountain	VA	3/17/2016	37.93	−79.128	737	0	0	8
South Ward Gap	WA	7/31/2016	46.177	−119.825	4184	0	2	100
Kahlotus	WA	8/22/2016	46.645	−118.633	9386	0	4	30
Starbuck	WA	7/18/2016	46.527	−118.087	2414	0	0	0
Eades Hollow	VA	11/21/2016	37.775	−78.851	1564	0	0	17
Rattlesnake	OR	7/24/2016	44.835	−121.118	9296	0	0	41
Table Rock	ID	6/30/2016	43.591	−116.131	2481	1	2	100
Cottonwood Ca	SD	10/16/2016	43.905	−101.862	41,775	0	2	0
Clifton	ID	8/23/2016	42.159	−112.01	2356	0	0	20
Henrys Creek	ID	8/21/2016	43.447	−111.765	52,988	0	8	125
Salvage	ID	6/24/2016	42.8	−114.669	1847	1	0	11
Rock	NV	7/29/2016	39.871	−119.896	2387	0	0	800
Metz	CA	5/22/2016	36.387	−121.217	3826	0	0	5
Bug Creek	AZ	6/28/2016	34.294	−112.117	1184	0	0	105
Longview	AZ	6/6/2016	31.633	−110.548	1105	0	0	40
Ridge	AZ	5/25/2016	31.529	−110.338	1391	0	0	53
Crutch	TX	3/23/2016	35.615	−101.117	45,052	0	4	0
Optima	OK	12/16/2016	36.692	−101.09	5084	0	0	0
Poplar	NC	3/31/2015	36.106	−82.337	768	0	0	3
Chestnut Knob	NC	11/6/2016	35.619	−81.657	6418	0	0	417
Horton	NC	11/22/2016	36.146	−81.568	1480	0	0	325
Bench Bluff	TN	11/12/2016	35.594	−85.242	1715	0	0	0
Pinnacle Mountain	SC	11/9/2016	35.055	−82.721	7869	0	1	1136
Rd 80	KS	3/17/2016	38.164	−96.391	63,061	0	0	0
Bar-Dew Lake	OK	3/19/2016	36.828	−96.039	14,806	0	0	62
Bear	OK	2/17/2016	36.309	−96.17	5966	0	0	80
Pawnee Cove	OK	2/18/2016	36.228	−96.411	3418	0	50	200
Pharoah	OK	2/18/2016	35.535	−96.097	13,579	0	14	50
Sand Creek	OK	2/18/2016	35.3	−96.104	3839	0	0	170
Double Header	OK	3/6/2016	35.35	−96.083	1413	0	0	15
Katie	OK	3/6/2016	35.258	−96.099	1573	2	0	35
Mustang	OK	3/6/2016	36.669	−96.025	10,060	0	0	82
Hall Horn	OK	3/16/2016	36.557	−96.298	5180	0	0	0
Walker	OK	3/19/2016	36.354	−96.235	2340	0	0	0
Varsity	OK	4/7/2016	35.728	−96.439	1216	0	0	55
Burmac	KS	3/23/2016	38.087	−97.668	10,668	12	11	0
Burley Hill	KS	4/5/2016	39.016	−96.645	16,381	1	0	0
Quinton Fire	OK	2/17/2016	35.14	−95.399	1219	0	0	5
Mason Fire	OK	2/19/2016	35.261	−95.473	1915	0	0	0
Round Prairie Road Fire	OK	2/19/2016	34.677	−95.173	2858	0	0	0
Cyclops	AL	11/5/2016	33.845	−87.033	660	0	0	4
Mount Pleasant	VA	11/19/2016	37.738	−79.178	11,001	0	0	120
Gap	CA	8/27/2016	41.856	−123.036	33,940	0	14	160
Willard	CA	9/11/2016	40.378	−120.749	2828	0	7	625
Kewa Fire	WA	8/2/2016	48.183	−118.284	1985	0	5	90

Incident Name	State	Ignition Date	Lat.	Long.	Acres Burned	Total Structures Damaged	Total Structures Destroyed	Total Structures Threatened
Cayuse Mtn	WA	8/22/2016	47.847	−118.038	9744	0	23	1535
Hart	WA	8/21/2016	47.822	−118.125	2819	20	40	605
Whit	WY	8/2/2016	44.409	−109.361	12,731	0	8	165
Cliff Creek	WY	7/17/2016	43.296	−110.382	36,131	0	1	135
Chimney	CA	6/1/2016	35.855	−118.025	1477	0	0	24
Erskine	CA	6/23/2016	35.569	−118.334	48,066	75	286	2500
Cedar	CA	8/16/2016	35.791	−118.571	29,191	0	12	2599
Slate	CA	10/4/2016	36.082	−118.556	2121	0	0	0
Meadow	CA	10/30/2016	35.975	−118.579	4346	0	0	0
Pioneer	ID	7/18/2016	44.139	−115.585	189,596	0	6	465
Roaring Lion	MT	7/31/2016	46.177	−114.248	8096	3	66	2347
Spokane Complex	WA	8/22/2016	47.492	−117.289	6839	2	17	303
Sherpa	CA	6/15/2016	34.497	−120.033	7549	0	5	271
Rey	CA	8/18/2016	34.586	−119.725	33,323	5	5	301
Pilot	CA	8/7/2016	34.308	−117.247	8267	0	0	5600
Blue Cut	CA	8/16/2016	34.324	−117.506	36,856	8	321	611
Bogart	CA	8/30/2016	33.986	−116.933	1475	0	2	426
Fish	CA	6/20/2016	34.181	−117.939	4528	0	0	869
Deer	CA	7/1/2016	35.222	−118.688	1885	0	0	300
Sage	CA	7/9/2016	34.366	−118.574	1002	1	0	2500
Little Valley	NV	10/14/2016	39.266	−119.839	2964	0	40	200
Cold	CA	8/3/2016	38.536	−122.077	6289	0	2	52
Trailhead	CA	6/28/2016	38.963	−120.83	5743	0	0	2600
Soberanes	CA	7/22/2016	36.322	−121.701	132,380	5	68	2010
Sand	CA	7/22/2016	34.391	−118.35	41,561	6	20	10,300
Clayton	CA	8/13/2016	38.915	−122.587	3792	29	302	1500
Loma	CA	9/26/2016	37.116	−121.818	4380	1	28	325
Border 3	CA	6/19/2016	32.611	−116.572	7958	3	17	1000
Mormon	AZ	5/15/2016	34.961	−111.573	7897	0	0	0
Goose	CA	7/30/2016	37.015	−119.466	2487	1	9	400
Tenderfoot	AZ	6/8/2016	34.232	−112.708	4363	0	3	300
Curry	CA	7/2/2016	36.087	−120.45	2837	0	0	25
Chimney	CA	8/13/2016	35.738	−121.075	46,950	24	70	1898
Juniper	AZ	5/20/2016	33.864	−110.926	32,293	1	0	141
Elk	AZ	7/21/2016	34.174	−109.864	1965	0	0	0
Beaver Creek	CO	6/19/2016	40.957	−106.505	44,221	0	17	131
Fulton	AZ	9/12/2016	34.281	−110.89	3237	0	0	296
Beulah Hill	CO	10/3/2016	38.07	−104.928	5769	0	14	750
Junkins	CO	10/17/2016	38.14	−105.136	19,023	0	26	745
Topock	AZ	4/6/2016	34.74	−114.51	1422	1	0	12
I40	TX	3/23/2016	35.244	−100.355	14,780	0	14	200
350 Complex	OK	4/5/2016	36.647	−99.266	58,055	0	0	825
Anderson Creek Fire	OK	3/23/2016	37.107	−98.835	374,523	0	54	10,000
Big Creek	MO	2/13/2016	36.634	−92.83	4031	0	0	0
Bob White	WV	4/3/2016	37.957	−81.7	824	0	0	10
Upper Conley Hollow	WV	4/4/2016	37.889	−82.095	1438	0	0	0
Jimmie Creek Rd	KY	10/26/2016	37.373	−82.386	500	0	0	0
Raven Rock	VA	11/2/2016	37.172	−82.61	2273	1	2	104
Bridge Creek Road	TN	10/30/2016	35.241	−85.559	1777	0	0	0
Spruce Pine Rd St Rt 7	KY	4/13/2016	37.522	−82.894	786	0	0	0
Little Shepherd Trail	KY	10/26/2016	36.951	−83.113	6751	0	0	0
Big Branch	KY	11/17/2016	37.062	−82.956	762	0	0	0
Poe Road	TN	11/11/2016	35.261	−85.254	758	0	0	0
Mowbray	TN	11/9/2016	35.286	−85.208	721	0	0	50
Bolts Br.	KY	11/24/2016	37.087	−83.656	1069	0	0	0
Lake Chinnabee	AL	11/28/2016	33.473	−85.871	1254	2	0	35
Caney Head	AL	3/20/2016	33.391	−85.843	957	0	0	0
Halls Top	TN	4/4/2016	35.875	−83.142	2464	1	1	71
Eagles Nest	KY	11/2/2016	37.53	−83.392	2857	0	0	50
Jetts Creek Fire	KY	11/6/2016	37.508	−83.563	3021	0	0	0
Bowlings Creek	KY	11/21/2016	37.361	−83.43	1023	0	0	0
Moore Peach	VA	4/10/2016	36.625	−82.986	1345	0	0	0

Incident Name	State	Ignition Date	Lat.	Long.	Acres Burned	Total Structures Damaged	Total Structures Destroyed	Total Structures Threatened
Sr116	TN	11/3/2016	36.169	−84.318	2222	0	0	0
Charles Branch Lane	TN	11/8/2016	36.204	−84.345	1071	0	0	0
Timber Ridge	GA	11/12/2016	34.828	−83.363	1002	0	0	400
Neddy Mountain Road	TN	11/11/2016	35.948	−83.072	788	0	0	150
Silver Mine	NC	4/21/2016	35.908	−82.791	6082	0	0	15
Party Rock	NC	11/5/2016	35.472	−82.241	8572	0	3	1050
State Line	TN	4/16/2016	35.926	−82.922	1111	0	0	17
Sr116-Devonia	TN	11/4/2016	36.116	−84.41	3077	0	0	0
Tellico	NC	11/3/2016	35.299	−83.589	14,172	0	1	336
Maple Springs	NC	11/4/2016	35.392	−83.932	7696	1	0	29
Dick's Creek	NC	10/23/2016	35.399	−83.249	833	0	0	31
Dobson 3	NC	11/8/2016	35.506	−83.244	741	0	0	50
Hwy 190	KY	11/2/2016	36.74	−83.724	957	0	0	0
Railroad Grade 2016	TN	4/18/2016	36.227	−82.113	1790	0	0	25
Kentucky Ridge	KY	11/7/2016	36.686	−83.858	1133	0	0	0
Old Roughy	NC	11/9/2016	35.371	−83.85	534	0	0	44
East Miller Cove	TN	11/17/2016	35.744	−83.799	1331	0	0	100
Quarry Creek	TN	11/16/2016	35.349	−84.281	643	0	0	9
Cobbly Nob	TN	11/28/2016	35.779	−83.342	732	23	108	0
Stinking Creek	TN	11/9/2016	36.453	−84.199	10,768	0	0	0
Boteler	NC	10/25/2016	35.068	−83.673	8626	0	0	314
Knob	NC	11/2/2016	35.114	−83.537	1132	0	0	0
Camp Branch	NC	11/23/2016	35.179	−83.558	3234	0	2	140
Wild Goose	LA	2/9/2016	31.406	−92.898	1260	0	3	20
Chimney Tops 2	TN	11/23/2016	35.687	−83.503	14,998	257	2066	2800
Knox Bell Line	KY	10/29/2016	36.907	−83.605	1272	0	0	0
Rock Mountain	GA	11/9/2016	34.99	−83.522	25,224	0	0	250
North Peak	NC	3/23/2016	35.753	−81.986	680	0	0	2
Old 50	FL	9/27/2016	28.547	−80.906	804	0	0	1
Island	FL	5/5/2016	29.318	−81.767	527	0	0	0
Skibo	MN	5/6/2016	47.498	−92.044	763	0	0	110
Clear Creek	NC	11/20/2016	35.72	−82.113	3493	0	0	392
Tombstone	NC	3/8/2016	35.545	−81.725	1747	0	0	0
Chetco Bar	OR	7/12/2017	42.238	−124.049	194,877	9	30	12,483
Helena	CA	8/31/2017	40.775	−123.062	18,709	8	141	5350
Canyon	CA	9/25/2017	33.861	−117.66	2740	6	0	1910
Canyon 2	CA	10/9/2017	33.823	−117.734	9102	58	26	5000
Minerva 5	CA	7/29/2017	39.903	−120.944	4545	0	0	395
Detwiler	CA	7/16/2017	37.55	−120.121	83,297	21	131	1500
Gate	CA	5/20/2017	32.654	−116.829	2265	0	0	315
Railroad	CA	8/29/2017	37.441	−119.613	12,765	0	19	511
Lilac 5	CA	12/7/2017	33.299	−117.203	4159	69	193	1500
Mission	CA	9/3/2017	37.236	−119.466	1006	8	9	250
Earthstone	NV	7/3/2017	39.591	−119.517	35,299	0	1	131
Preacher	NV	7/24/2017	38.855	−119.588	5330	0	0	800
Prater	NV	8/6/2017	39.551	−119.669	1572	0	0	30
Long Valley	CA	7/11/2017	39.992	−119.92	80,456	3	10	500
Winnemucca Ranch	NV	7/4/2017	39.756	−119.644	4153	0	5	300
Cold Springs	NV	7/14/2017	39.646	−119.938	1557	0	0	100
Opera	CA	4/30/2017	33.997	−117.301	1070	0	0	0
Cutter	NV	10/3/2017	38.829	−119.604	4065	0	0	150
Roadrunner	CA	7/30/2017	36.015	−118.933	2436	0	0	10
Pier	CA	8/29/2017	36.122	−118.708	36,626	0	2	1360
Winter	CA	7/6/2017	38.526	−122.054	2485	0	0	63
Atlas	CA	10/9/2017	38.364	−122.237	51,664	129	790	5000
Jones	OR	8/11/2017	44.004	−122.512	10,260	0	1	5
Nuns	CA	10/9/2017	38.349	−122.503	56,883	0	0	0
Hatchery	NV	7/4/2017	38.977	−114.091	1142	0	0	0
Creek	CA	12/5/2017	34.294	−118.352	15,833	81	123	2500
East Fork	MT	8/27/2017	48.231	−109.576	21,165	5	5	80
Rye	CA	12/5/2017	34.43	−118.635	4895	3	6	5460
Gibralter Ridge	MT	8/8/2017	48.86	−114.849	6299	0	1	145
Caribou	MT	8/11/2017	48.979	−115.351	28,101	0	40	570

Incident Name	State	Ignition Date	Lat.	Long.	Acres Burned	Total Structures Damaged	Total Structures Destroyed	Total Structures Threatened
West Fork	MT	8/30/2017	48.519	−115.606	21,154	0	0	709
Canyon Creek	WA	7/15/2017	48.271	−120.072	1232	0	2	85
East Saddle	WA	8/12/2017	46.782	−119.349	17,318	2	2	40
Wall	CA	7/7/2017	39.463	−121.406	6488	12	91	5400
Cascade	CA	10/9/2017	39.359	−121.375	16,155	0	200	1000
Cherokee	CA	10/9/2017	39.591	−121.585	8415	0	3	53
Tubbs	CA	10/9/2017	38.568	−122.68	36,981	14	576	29,192
Sulfur	CA	10/9/2017	38.992	−122.666	2591	70	205	1720
Oil Well	NV	7/17/2017	40.92	−115.725	7240	0	28	200
Redwood Valley Incident	CA	10/9/2017	39.339	−123.213	36,545	0	90	100
Pocket	CA	10/9/2017	38.77	−122.883	18,691	0	0	0
Palmer	CA	9/2/2017	33.991	−117.121	4148	1	0	150
Mecca Fire	OR	6/26/2017	44.781	−121.231	2515	0	0	23
Emerson 0638 Rn	OR	7/25/2017	44.69	−121.012	10,683	0	1	25
Thomas	CA	12/4/2017	34.459	−119.303	281,982	280	1063	18,000
Nena Springs	OR	8/9/2017	44.974	−121.198	70,074	4	10	199
Pilot Valley	NV	8/13/2017	41.106	−114.095	2578	2	6	157
Ana	OR	7/8/2017	43.009	−120.769	5801	2	4	55
Eagle Creek	OR	9/2/2017	45.618	−121.942	48,816	0	9	5526
Sheep Gap	MT	8/29/2017	47.475	−115.046	24,702	0	0	80
Silver Dollar	WA	7/2/2017	46.57	−119.779	30,789	0	0	30
Horn Butte 0594 Rn	OR	7/21/2017	45.682	−120.069	9325	0	0	35
Glade 3	WA	7/30/2017	46.144	−120.054	10,582	0	1	20
Morgan Creek	OR	8/3/2017	44.426	−117.235	2329	0	0	0
Martin Canyon	ID	7/23/2017	43.49	−114.168	4053	0	0	0
Lagoon	ID	7/26/2017	42.955	−114.438	1484	0	3	10
Mammoth Cave	ID	8/4/2017	43.155	−114.193	50,391	0	3	50
Breeze	ID	6/26/2017	43.302	−115.87	1863	0	0	40
North Delphia	MT	7/14/2017	46.548	−108.278	3767	0	0	40
Sage Hills	MT	7/20/2017	45.763	−108.348	1197	0	0	100
Lincoln Beach	UT	6/23/2017	40.071	−111.842	2298	0	0	14
Mulberry	AZ	5/6/2017	31.901	−110.611	1846	0	4	20
Lizard	AZ	6/7/2017	31.986	−110.006	15,791	0	0	108
Encino	AZ	6/21/2017	31.65	−110.648	1357	2	15	250
Cajete	NM	6/15/2017	35.809	−106.559	1433	0	0	233
Sawmill	AZ	4/23/2017	31.822	−110.687	47,357	0	0	415
Alice Creek	MT	7/22/2017	47.142	−112.438	29,971	0	4	240
Sunrise	MT	7/17/2017	47.07	−114.838	26,896	0	0	382
Tarina	CA	6/30/2017	35.385	−118.793	1257	0	0	6
Lolo Peak	MT	7/15/2017	46.666	−114.242	62,316	2	10	1962
Mendenhall	MT	8/26/2017	45.653	−110.18	1196	0	2	30
July	MT	7/3/2017	47.89	−108.575	11,409	0	6	101
Hondito	NM	5/15/2017	36.608	−106.02	6949	0	0	0
Hill	CA	6/26/2017	35.405	−120.481	1900	5	4	30
Wolf	SD	3/4/2017	43.998	−102.169	1797	0	0	45
Hodgeman County	KS	3/6/2017	38.143	−99.853	8518	9	8	0
South Wenas	WA	6/27/2017	46.72	−120.601	2956	0	0	175
Spartan	WA	6/26/2017	47.32	−120.155	8775	0	0	91
Sheep	WA	7/24/2017	46.758	−120.544	1564	0	0	0
Monument Hill	WA	8/17/2017	47.304	−119.718	6437	19	23	175
Meyers	MT	7/14/2017	45.989	−113.552	68,711	0	1	344
Jolly Mountain	WA	8/11/2017	47.341	−120.978	38,159	0	0	5624
Rattlesnake Hills	WA	7/6/2017	46.515	−120.432	3553	0	0	30
Perryton	TX	3/6/2017	35.99	−100.36	290,211	0	11	200
Monitor	WA	11/1/2017	47.503	−120.4	1196	0	0	300
Brianhead	UT	6/17/2017	37.788	−112.693	74,276	5	26	1526
Thirty Seven	CA	10/9/2017	38.155	−122.474	1773	4	0	80
303	TX	2/28/2017	33.401	−102.535	9601	0	0	0
Slinkard	CA	8/29/2017	38.659	−119.571	8814	0	0	510
Keystone	WY	7/3/2017	41.174	−106.281	2784	0	1	80
Tripp	TX	2/10/2017	34.448	−100.789	2573	0	0	4
Dumas Complex	TX	3/6/2017	35.357	−101.722	26,155	0	0	150

Incident Name	State	Ignition Date	Lat.	Long.	Acres Burned	Total Structures Damaged	Total Structures Destroyed	Total Structures Threatened
Prison	TX	2/28/2017	34.522	−101.804	2420	4	13	1143
2018 North Sargent Wf	TX	10/16/2017	28.813	−95.62	3959	0	0	60
Oks—283	OK	3/7/2017	36.689	−99.755	68,558	0	0	300
Lefors East	TX	3/7/2017	35.365	−100.524	68,701	0	0	0
Beaver Mountain	OK	1/31/2017	35.168	−95.339	4754	0	0	0
Powder Mill	OK	2/2/2017	34.964	−95.382	1551	0	0	47
Highlands	KS	3/7/2017	38.182	−97.919	7418	9	13	1100
Jupiter Hills	KS	3/4/2017	38.109	−97.848	1283	1	1	100
Legion Lake	SD	12/11/2017	43.669	−103.394	54,868	0	3	203
Sugar Cove	NC	1/28/2017	35.75	−82.143	638	0	0	14
Turn Table Fire	SC	4/2/2017	33.312	−79.878	1868	0	0	0
Dobson Knob	NC	4/9/2017	35.812	−81.993	1720	0	0	45
Big Branch Fire	KY	4/9/2017	37.181	−83.054	651	0	0	32
Ne 212th St	FL	3/31/2017	29.469	−81.956	610	0	0	40
Sod Farm 2	FL	4/16/2017	28.913	−81.453	901	0	0	0
Lost Creek	OK	3/3/2017	35.403	−96.141	2420	0	0	25
Spocogee	OK	3/1/2017	36.071	−96.33	6318	0	0	45
Gun Range	OK	3/21/2017	35.646	−96.063	1524	0	0	3
Cod Dr	FL	7/8/2017	28.767	−82.258	640	0	0	12
Conner	FL	3/26/2017	29.252	−81.918	676	0	0	10
310 West Of Como	MS	1/29/2017	34.518	−90.075	745	2	1	6
Cr630 E	FL	2/15/2017	27.782	−81.315	5096	0	142	0
Oks—Starbuck	OK	3/7/2017	37.081	−99.893	657,299	0	0	1000
Bonita	NM	6/3/2017	36.58	−106.149	7754	0	0	65
Garfield Road	FL	3/22/2017	30.418	−82.022	721	14	21	3
West Mims	GA	4/6/2017	30.651	−82.294	166,737	0	4	920
Apple	CA	6/9/2018	39.924	−122.349	2849	0	9	0
Creek	CA	6/24/2018	40.486	−122.518	1353	0	11	610
Middle Ridge	OK	3/21/2017	35.577	−94.626	8501	0	0	0
Persimmon Ridge	OK	3/21/2017	35.653	−95.088	5333	0	0	0
Sun	CA	10/7/2018	40.23	−122.143	3921	0	0	70
Lost Fire	OK	3/21/2017	34.708	−95.757	4178	0	2	4
Potato Hills	OK	3/23/2017	34.694	−95.226	2503	0	0	0
Montecito	WA	6/28/2018	46.175	−119.762	1877	0	0	50
Wagon Wheel	WA	9/1/2018	46.35	−119.513	4063	0	0	90
Milepost Twenty Two	WA	6/20/2018	46.966	−120.05	7406	0	0	16
Boffer	WA	8/11/2018	46.142	−119.141	4645	0	7	0
Conrad	WA	7/1/2018	46.739	−120.665	4611	0	1	220
Milepost 90	WA	8/1/2018	45.681	−120.937	10,757	0	0	70
Lee Williams Rd	FL	3/5/2017	26.133	−81.637	7288	1	6	1000
South Valley Road	OR	8/1/2018	45.371	−121.161	20,471	0	19	212
Jackson Ranch	OK	3/23/2017	35.797	−96.217	4243	0	0	40
Substation 0730 Rn	OR	7/17/2018	45.5	−120.939	69,109	8	52	1363
Mile Marker 44	WA	9/1/2018	46.149	−120.529	4063	0	0	0
Boxcar 0410 Rn	OR	6/21/2018	45.022	−121.004	99,874	0	0	55
Tenino Fire	OR	8/16/2018	44.708	−121.371	8821	0	0	0
Graham 0420 Od	OR	6/21/2018	44.55	−121.4	2102	0	11	204
Angel Springs	WA	8/2/2018	47.775	−118.029	4718	0	14	170
Eagle	CA	7/13/2018	41.268	−120.105	2116	0	0	18
Soap Lake	WA	6/11/2018	47.436	−119.49	2158	0	0	35
Chelan Hills	WA	7/27/2018	47.782	−119.962	1850	4	8	100
Rocky Reach	WA	7/13/2018	47.527	−120.327	3346	0	0	313
Boylston	WA	7/19/2018	46.85	−120.11	66,292	1	6	1
Keithly	ID	7/25/2018	44.464	−116.843	17,588	0	0	31
Silver State	NV	7/14/2018	40.886	−115.665	3766	0	0	0
Rocky	NV	6/23/2018	40.378	−118.262	1641	1	1	10
Owyhee	NV	7/21/2018	41.948	−116.077	5347	0	0	60
South Sugarloaf	NV	8/17/2018	41.716	−116.019	241,426	3	17	116
Goodwin	AZ	6/24/2017	34.381	−112.299	28,192	3	33	1400
La Tuna	CA	9/1/2017	34.23	−118.316	7035	1	10	1376
Powerline	ID	8/4/2017	42.699	−112.605	54,378	0	1	35
White Creek	NC	3/16/2017	35.837	−81.883	4166	0	0	7
Shoestring	ID	8/5/2017	42.878	−114.574	35,543	0	1	2
Penn Swamp Fire	NJ	7/20/2017	39.677	−74.638	3587	0	0	0

Incident Name	State	Ignition Date	Lat.	Long.	Acres Burned	Total Structures Damaged	Total Structures Destroyed	Total Structures Threatened
Weogufkee	OK	3/20/2017	35.233	−95.904	2226	0	0	0
Holiday	FL	4/5/2017	26.003	−80.468	8858	0	0	20
30th Ave	FL	4/20/2017	26.177	−81.605	6463	18	14	3884
Powerline	WY	8/12/2018	44.461	−108.926	1837	0	0	0
Raintree Blvd	FL	5/13/2017	27.074	−82.052	3319	0	0	0
Flat Rock Fire	NY	7/12/2018	44.87	−73.637	658	0	0	2
Tye River	VA	5/3/2018	37.905	−79.154	1761	0	0	29
Spring Creek	CO	6/27/2018	37.543	−105.144	107,108	119	225	2878
Blaine	CA	8/13/2017	33.984	−117.29	1117	46	0	441
Roosevelt	WY	9/15/2018	43.06	−110.387	55,330	1	57	1153
8 Mile	ID	9/22/2018	42.595	−111.54	1001	0	5	95
Miles	OR	7/16/2018	42.828	−122.699	40,343	0	2	1011
Ramsey Canyon	OR	8/22/2018	42.587	−122.992	2127	0	1	540
Natchez	CA	7/15/2018	41.895	−123.566	38,800	0	0	104
Taylor Creek	OR	7/15/2018	42.488	−123.619	57,505	0	0	3292
Klondike	OR	7/16/2018	42.418	−123.873	178,311	0	0	1940
Ferguson	CA	7/13/2018	37.635	−119.807	97,307	0	11	5236
Kerlin	CA	9/4/2018	40.625	−123.512	1775	0	5	100
Hirz	CA	8/9/2018	40.984	−122.279	46,700	0	1	171
Delta	CA	9/5/2018	41.007	−122.462	63,732	7	45	330
River	CA	7/27/2018	39.055	−123.019	48,920	0	2	305
County	CA	6/30/2018	38.683	−122.155	92,450	4	31	1516
Nelson	CA	8/10/2018	38.312	−121.999	2205	1	1	260
Whaleback	CA	7/27/2018	40.627	−120.824	18,640	0	0	460
Hat	CA	8/9/2018	40.998	−121.489	1971	0	0	380
Boyds	WA	8/11/2018	48.632	−118.154	5196	0	10	529
Crescent Mountain	WA	7/29/2018	48.384	−120.446	53,258	0	0	1196
Camp	CA	11/8/2018	39.748	−121.565	153,687	751	18,838	17,500
Stone	CA	8/15/2018	41.425	−121.013	39,455	0	2	119
Chaves	NV	6/3/2018	39.3	−119.412	3652	1	0	98
Upper Colony	NV	6/17/2018	38.812	−119.411	1255	0	0	92
Donnell	CA	8/1/2018	38.383	−119.822	36,151	0	136	305
Rattlesnake Creek	ID	7/23/2018	45.232	−116.376	8461	0	0	618
Rabbit Foot	ID	8/2/2018	44.848	−114.23	33,787	0	0	1446
Pinery	AZ	5/12/2018	31.982	−109.353	1474	0	0	25
Viewpoint	AZ	5/11/2018	34.693	−112.343	5389	14	0	0
Tinder	AZ	4/27/2018	34.59	−111.11	16,083	0	96	1700
Hub Point	AZ	7/27/2018	34.251	−110.29	4674	0	0	0
Soldier Canyon	NM	6/7/2018	33.185	−105.759	1386	0	0	100
Pierson	NM	4/17/2018	32.499	−103.418	1060	0	0	2
Ute Park	NM	5/31/2018	36.533	−105.028	30,177	3	15	2952
Valley	CA	7/6/2018	34.105	−116.946	1250	0	0	500
Harbor Bay	TX	4/13/2018	35.619	−101.631	1428	0	8	50
Cranston	CA	7/25/2018	33.715	−116.705	13,096	6	12	6230
Holy	CA	8/6/2018	33.704	−117.468	22,845	18	24	13,300
Stone	CA	6/4/2018	34.55	−118.292	1659	0	0	150
Badger Hole	CO	4/17/2018	37.433	−102.088	49,146	1	24	0
Charlie	CA	9/22/2018	34.521	−118.559	3367	0	0	100
Cr 26	TX	4/14/2018	35.256	−100.084	1386	0	0	6
Milliron	TX	4/13/2018	34.913	−100.011	20,437	0	21	75
34 Complex	OK	4/12/2018	36.585	−99.352	57,533	0	55	150
Hill	CA	11/8/2018	34.207	−118.953	4427	2	4	437
Front	CA	8/19/2018	35.119	−120.097	1126	0	0	5
Perry	NV	7/27/2018	39.802	−119.496	53,734	3	16	418
Airline	CA	6/4/2018	36.391	−120.962	1477	0	0	1
Lake Christine	CO	7/3/2018	39.419	−107.037	12,506	9	6	1329
Chateau	CO	6/29/2018	38.815	−105.3	1414	0	8	754
Carson Midway	CO	3/16/2018	38.527	−104.716	4773	0	2	0
Rhea	OK	4/12/2018	36.003	−99.003	277,949	0	50	3500
Organ	NM	6/24/2018	32.454	−106.527	4880	0	0	1
Harman Road	TX	7/18/2018	31.333	−97.972	3094	0	1	115
Owl Creek	NV	8/30/2018	40.658	−115.526	1165	0	0	12

Incident Name	State	Ignition Date	Lat.	Long.	Acres Burned	Total Structures Damaged	Total Structures Destroyed	Total Structures Threatened
Lime Rock Rd (19)	FL	6/24/2018	29.765	−84.866	1190	4	36	400
Cougar Creek	WA	7/28/2018	47.816	−120.478	42,681	0	0	3000
Rozell	MO	2/15/2018	36.587	−92.862	1970	0	6	0
Bald Mountain	UT	8/24/2018	39.925	−111.693	21,016	0	1	2600
Pole Creek	UT	9/6/2018	39.982	−111.53	102,426	0	1	2626
Hill Top	UT	8/6/2018	39.737	−111.441	1784	2	4	320
Dollar Ridge	UT	7/1/2018	40.111	−110.877	69,817	6	453	1023
Little Shepherds Trail	KY	5/1/2018	36.976	−83.034	541	0	0	0
Keepers Branch Fire	SC	3/4/2018	33.189	−79.542	819	0	0	6
Range Two	NV	9/30/2018	40.669	−115.448	9361	0	8	60
Dog Head	NM	6/14/2016	34.851	−106.3	19,816	0	73	1950
Ranch	CA	7/27/2018	39.269	−122.775	427,048	0	0	86
416	CO	6/1/2018	37.493	−107.903	55,123	0	0	3386
Grass Valley	WA	8/11/2018	47.94	−119.166	76,074	1	20	330
West 60	OK	3/7/2018	36.789	−96.487	18,715	0	0	10
Carr	CA	7/23/2018	40.715	−122.593	233,710	282	1608	5013
Badger Creek	WY	6/10/2018	41.055	−106.11	20,752	4	3	553
Tomahawk	AR	4/12/2018	36.056	−92.671	533	0	8	15
Woolsey	CA	11/8/2018	34.125	−118.824	97,962	365	1643	57,000
Flag Pond (11)	FL	3/21/2018	26.139	−81.595	2562	0	0	0
Buffalo Corral	AZ	7/14/2019	31.573	−110.377	1144	0	0	0
Kincade	CA	10/23/2019	38.672	−122.776	77,785	60	375	90,015
Easy	CA	10/30/2019	34.267	−118.829	2105	1	1	2635
Sandalwood	CA	10/10/2019	33.999	−117.084	1048	16	76	0
Tick	CA	10/24/2019	34.451	−118.394	4932	48	31	10,425
Maria	CA	11/1/2019	34.314	−119.066	10,036	0	5	2722
Saddleridge	CA	10/10/2019	34.318	−118.515	9656	93	38	25,760
Black Bridge	CO	4/4/2019	38.074	−103.177	1690	0	0	7
116th Ave Se (11)	FL	3/21/2018	26.034	−81.56	29,262	0	3	0
335	TX	4/13/2018	32.676	−99.716	2481	0	15	100
Blue Creek #2	OK	3/14/2018	35.052	−95.594	2578	0	0	0
Deerte	OK	3/15/2018	35.367	−95.871	1833	0	0	8
Henry	OK	3/20/2018	35.581	−96.42	1160	0	0	17
Brewster	OK	3/16/2018	35.685	−96.299	4049	0	0	20
Flying G	OK	3/12/2018	36.124	−96.203	1886	0	0	184
Walker	OK	3/24/2018	36.35	−96.233	2626	0	0	9
Drumb	OK	3/24/2018	36.467	−96.3	30,419	0	0	9
Onion Prairie	OK	3/6/2018	36.641	−96.017	3911	0	0	20
New Years Wf	TX	1/1/2018	29.706	−93.908	5613	0	0	12
Farmers Road	TX	1/22/2018	32.738	−97.596	2379	0	0	252
Carbon	TX	4/13/2018	35.214	−100.068	12,148	0	0	500
Pemberton	AZ	8/6/2019	34.731	−112.676	1211	0	0	0
Green Ravine	UT	9/3/2019	40.683	−112.228	2260	0	0	3
Goose Point	UT	8/21/2019	40.076	−111.832	9190	0	0	23
Dove	AZ	5/24/2019	33.799	−112.429	1078	0	0	10
White Wing	AZ	5/30/2019	33.796	−112.437	1797	0	0	30
Tenaja	CA	9/4/2019	33.549	−117.258	1820	2	0	1200
Walker	CA	9/4/2019	40.09	−120.585	58,752	0	9	78
Long Valley	CA	8/24/2019	39.882	−119.995	2451	4	1	80
Briceburg	CA	10/6/2019	37.608	−119.932	5555	0	1	160
Woodbury	AZ	6/8/2019	33.52	−111.175	130,243	0	0	1537
Stuckey Rd Ma	MT	9/2/2019	47.586	−111.357	4077	0	9	0
Matson	WA	10/7/2019	46.619	−118.93	8715	0	0	86
Sand	CA	6/8/2019	38.904	−122.259	2473	0	7	125
Museum	AZ	7/21/2019	35.263	−111.62	2011	0	0	0
Elmer City	WA	6/23/2019	48.064	−118.943	1996	2	2	45
Desert Canyon	WA	7/23/2019	47.711	−120.148	1505	0	0	16
243 Command	WA	6/4/2019	46.855	−119.785	18,891	1	2	36
Cut Across	MT	4/7/2019	45.63	−106.7	1858	0	0	130
Boulder	CA	6/5/2019	35.32	−119.93	1199	0	0	0
Decker	CO	9/8/2019	38.441	−105.995	9876	0	4	142
Boulin	AZ	8/6/2019	35.382	−112.036	4094	0	0	12
Coldwater	AZ	5/30/2019	34.481	−111.335	16,824	0	0	14

Incident Name	State	Ignition Date	Lat.	Long.	Acres Burned	Total Structures Damaged	Total Structures Destroyed	Total Structures Threatened
Cave	CA	11/25/2019	34.489	−119.768	2761	1	0	15,000
Left Hand	WA	7/23/2019	46.915	−120.975	3234	0	0	347
North Hills	MT	7/26/2019	46.765	−111.944	4144	0	0	600
Tx Point East Christmas Eve	TX	12/24/2019	29.716	−93.9	1163	0	0	43
Williams Flats	WA	8/2/2019	47.977	−118.498	44,680	0	3	56
Pedro Mountain	WY	8/24/2019	42.337	−106.826	21,910	0	8	90
Cove Creek	ID	8/4/2019	45.346	−114.465	5273	0	0	39
Channing	TX	2/16/2019	35.663	−102.275	7855	0	0	20
Burnside	OK	3/19/2019	34.593	−97.029	1117	0	0	10
East Kennedy Creek	KS	4/2/2019	38.29	−95.815	1003	0	0	0
Clark Branch #2	KY	9/17/2019	37.603	−82.621	1315	0	0	0
344 D	FL	9/11/2019	30.356	−84.632	2339	0	0	0
Cr 2297 Allenton (03)	FL	3/30/2019	30.115	−85.482	725	0	0	52
Dry Hollow	WV	11/28/2019	38.831	−79.308	1412	0	0	16
Kennedy Peak	VA	11/14/2019	38.762	−78.466	769	0	0	0
Spring Hill Fire	NJ	3/30/2019	39.79	−74.451	8182	0	0	0

Appendix D. 2052 Weather Time Series Estimation

We used these publicly-available online repositories of NOAA RTMA data:

1. Iowa state (Iowa State) [57] covering 2011-current
2. National Centers for Environmental Information (NCEI) National Digital Guidance Database (NDGD) (NOAA NCEI, 2022) covering 2011- current

Since approximately 3% to 4% of hourly records are missing from both the Iowa State and NCEI datasets, we merged these datasets to minimize the amount of missing data.

Mid-century fire weather inputs were generated by scaling or "nudging" 2011–2020 Real Time Mesoscale Analysis (RTMA) temperature, relative humidity, and precipitation by computing distribution changes between 2021 and 2051 ensemble regional model output. While wind is an essential fire weather variable, it was excluded from nudging because the literature does not support a statistically robust climate change signal for it (e.g., Torralba et al., 2017 [58]).

We used the Multivariate Adaptive Constructed Analogs (MACA) version 2 as our source for 2020 and 2050 calibration data because it demonstrates skillful performance for fire weather variables, particularly relative humidity and wind (Abatzoglou and Brown, 2012 [33]). MACA is statistically downscaled Coupled Model Intercomparison Project version 5 (CMIP5; Taylor et al., 2012 [32]) available in a ~4-km grid over the contiguous United States (CONUS). It is available at daily resolution and at temporal ranges for present-day conditions (1950–2005) and future experiments under Representative Concentration Pathways (RCPs) 4.5 and 8.5. RCP4.5, which represents an intermediate scenario, was used for this experiment. Temporal ranges for the "2020" and "2050" calibration data were defined as 2011–2020 and 2048–2057 ensemble means, respectively. Note that the CCSM4 MACA ensemble member was not included in order to maintain consistency across variables, because it was not available for relative humidity at the MACA Data Portal (https://climate.northwestknowledge.net/MACA/data_portal.php, accessed on 8 August 2022).

Nudging was performed independently at each geographic grid point. In order to facilitate this, the 4-km rectilinear MACA data had to be interpolated to the 2.5-km curvilinear RTMA grid. The National Center for Atmospheric Research Command Language (NCL)'s regridding package from the Earth System Modeling Framework was used (https://www.ncl.ucar.edu/Applications/ESMF.shtml, accessed on 8 August 2022). We used bilinear interpolation for temperature and relative humidity, and conservative regridding for precipitation since it does not represent a smoothly varying field.

Nudging code was obtained from the bias_correction Python3 package (https://github.com/pankajkarman/bias_correction, accessed on 8 August 2022). Bias correction

techniques like those employed here are used to correct modeled projections by adjusting them with statistical scaling factors derived between historical model output and observations; put another way, they are used to downscale climate change projections to station locations (e.g., Fang et al., 2015 [59], Luo et al., 2018 [60]). Likewise, we use them here to nudge RTMA output with respect to scaling factors computed between 2020 and 2050 MACA output. We summarize the techniques here.

Appendix D.1. Precipitation

RTMA precipitation projections were obtained via gamma distribution mapping, a technique developed by Switanek, et al., 2017 [61]). Gamma distribution mapping is unlike other bias correction methods because it accounts for the frequency of rain days and the likelihood of events (Switanek, et al., 2017 [61]).

After summing hourly RTMA precipitation into daily accumulations to match the temporal resolution of the MACA data, this procedure goes as follows:

1. Define rain days (RDs) as those which feature non-zero precipitation accumulations for each distribution. Then compute the expected number of projected 2050 RTMA rain days (RDP):
$$RD_P = RD_{RTMA} \times \frac{RD_{MACAF}}{RD_{MACAH}} \quad \text{(A1)}$$
where RDRTMA, RDMACAF, and RDMACAH are the number of rain days in RTMA, 2050 MACA, and 2020 MACA data, respectively. In the event MACA 2050 has fewer RDs than MACA 2020, this results in a downward adjustment in RDs in the nudged RTMA distribution. Note that projected RTMA RDs can never increase above original RTMA RDs, an important limitation in this approach.
2. Fit gamma probability density functions (PDFs) to each of the modeled rain-day distributions. Cumulative distribution functions (CDFs) and their inverses (ICDFs) are found from these PDFs.
3. Calculate the relative scaling (SFR) between the fitted RTMA and 2020 MACA distributions at all CDF values corresponding to the precipitation events of the RTMA time series:
$$SF_R = \frac{ICDF_{RTMA}(CDF_{RTMA})}{ICDF_{MACAH}(CDF_{RTMA})} \quad \text{(A2)}$$
where SFR is an array of relative scaling factors, ICDFRTMA and ICDFMACAH are the ICDFs for the fitted 2020 RTMA and MACA distributions, respectively, and CDFRTMA is the estimated CDF for RTMA precipitation values. As an example, say the largest value in the RTMA time series is equal to 40 mm and corresponds to a CDF value of 0.997 (in other words, ICDFRTMA(0.997) will yield 40 mm), but ICDFMACAH(0.997) yields only 6 mm (we discuss these systematic magnitude discrepancies in Assumptions and Limitations). The most extreme nudged value will have a relative scaling factor of 6.67 (40/6).
4. Calculate recurrence intervals (RIs) from the three fitted CDFs, then find the adjusted RI for 2020 RTMA:
$$RI_{SC} = max\left(1, \frac{RI_{MACAF} \times RI_{RTMA}}{RI_{MACAH}}\right) \quad \text{(A3)}$$
where RIMACAF, RIRTMA, and RIMACAH correspond to the RIs for the RTMA and 2050 and 2020 MACA data, respectively. The value is always greater than or equal to 1 to ensure that the subsequent step yields values between 0 and 1. This step adjusts the RI of 2050 MACA events by differences in the extremity of 2020 RTMA and MACA events. For example, if the RI for the most extreme 2020 RTMA value is shorter than that of the most extreme 2020 MACA value, then the RI for the most

extreme 2050 MACA value will be shortened accordingly. RISC is then used to find the corresponding scaled CDF values with

$$CDF_{SC} = 1 - \frac{1}{RI_{SC}} \tag{A4}$$

where CDFSC reflects the scaling of the change in MACA event likelihoods between 2050 and 2020 with respect to RTMA likelihoods.

5. The initial array of projected RTMA values is:

$$RTMA_I = ICDF_{MACAF}(CDF_{SC}) \times SF_R \tag{A5}$$

where ICDFMACAF is the ICDF for the 2050 MACA data. In the event that (A1) adjusted the RDs for the projected time series, RTMAI is linearly interpolated along the adjusted length of RDP.

6. The array of projected values is then placed back into the RTMA time series at the corresponding locations. For example, if the largest annual RTMA value occurred on April 21st, then the largest projected RTMA value will be placed on that same day.
7. Last, the ratio between the projected and original RTMA values for each day is applied to the hourly RTMA precipitation time series.

Appendix D.2. Temperature

RTMA temperature projections were obtained via a normal distribution mapping technique (Switanek, et al., 2017 [61]). After applying cubic spline interpolation to daily minimum and maximum MACA temperatures to obtain hourly distributions (we discuss this further in Assumptions and Limitations), the steps go as follows:

1. All three distributions are linearly detrended to get a more accurate measure of the natural variability. While trends are added back at the end, all subsequent steps use the detrended time series.
2. Gaussian PDFs are fit to each of the annual distributions, then corresponding CDFs and ICDFs are derived from these.
3. An absolute scaling factor is found:

$$SF_A = [ICDF_{RTMA}(CDF_{RTMA}) - ICDF_{MACAH}(CDF_{MACAH})] \times \left(\frac{\sigma MACAF}{\sigma MACAH}\right) \tag{A6}$$

where σMACAF and σMACAH are the standard deviations of the 2050 and 2020 MACA data and all other terms are defined as before.

4. RIs are calculated from the CDFs, scaled with (A3), then used to find the modified CDF with

$$CDF_{SC} = 0.5 + sgn(CDF_{MACAF} - 0.5) \times \left|0.5 - \frac{1}{RI_{SC}}\right| \tag{A7}$$

Equation (A7) differs from (A4) because the normal distribution is two-tailed.

5. The initial array of projected RTMA values is

$$RTMA_I = ICDF_{MACAF}(CDF_{SC}) + SF_A \tag{A8}$$

6. As before, reinsert projected values into the original RTMA time series. Then add the trend of the RTMA time series back into the projected one.

Appendix D.3. Relative Humidity

Mid-century relative humidity projections used a comparatively simpler approach called empirical quantile mapping (Gudmundsson et al., 2012 [62]). Unlike the previous two methods, it makes no assumptions about the underlying distribution of the data. Briefly, it goes as follows:

1. An empirical CDF (ECDF) is approximated for the 2020 MACA distribution.

2. The corresponding percentiles from the ECDF are found in the RTMA data.
3. The difference between the value at each equivalent percentile is computed between the 2050 and 2020 MACA data.
4. This difference is applied to the RTMA data.

In this way, the order of observations in the 2020 record is maintained (i.e., underlying variability) while shifting towards a future climate.

References

1. Burke, W.D.; Tague, C.; Kennedy, M.C.; Moritz, M.A. Understanding How Fuel Treatments Interact With Climate and Biophysical Setting to Affect Fire, Water, and Forest Health: A Process-Based Modeling Approach. *Front. For. Glob. Chang.* **2021**, *3*, 143. [CrossRef]
2. Westerling, A.L.; Hidalgo, H.G.; Cayan, D.R.; Swetnam, T.W. Warming and earlier spring increase western US forest wildfire activity. *Science* **2006**, *313*, 940–943. [CrossRef]
3. Vose, J.M.; Peterson, D.L.; Domke, G.M.; Fettig, C.J.; Joyce, L.A.; Keane, R.E.; Luce, C.H.; Prestemon, J.P.; Band, L.E.; Clark, J.S.; et al. Forests. In *Impacts, Risks, and Adaptation in the United States: Fourth National Climate Assessment, Volume II*; Reidmiller, D.R., Avery, C.W., Easterling, D.R., Kunkel, K.E., Lewis, K.L.M., Maycock, T.K., Stewart, B.C., Eds.; U.S. Global Change Research Program: Washington, DC, USA, 2018; pp. 232–267. [CrossRef]
4. Western Forestry Leadership Coalition. The True Cost of Wildfire in the Western U.S. 2010. Available online: https://www.blm.gov/or/districts/roseburg/plans/collab_forestry/files/TrueCostOfWilfire.pdf (accessed on 1 January 2020).
5. NOAA National Centers for Environmental Information. 2022. Available online: https://www.ncei.noaa.gov/has/HAS.FileAppRouter?datasetname=9950_01&subqueryby=STATION&applname=&outdest=FILE (accessed on 1 January 2020).
6. Abatzoglou, J.T.; Williams, A.P. Impact of anthropogenic climate change on wildfire across western US forests. *Proc. Natl. Acad. Sci. USA* **2016**, *113*, 11770–11775. [CrossRef] [PubMed]
7. Radeloff, V.C.; Helmers, D.P.; Kramer, H.A.; Mockrin, M.H.; Alexandre, P.M.; Bar-Massada, A.; Butsic, V.; Hawbaker, T.J.; Syphard, A.D.; Stewart, S.I. Rapid Growth of US Wildland-Urban Interface Raises Wildfire Risk. *Proc. Natl. Acad. Sci. USA* **2018**, *115*, 3314–3319. [CrossRef]
8. Caggiano, M.D.; Hawbaker, T.J.; Gannon, B.M.; Hoffman, C.M. Building loss in wui disasters: Evaluating the core components of the wildland–urban interface definition. *Fire* **2020**, *3*, 73. [CrossRef]
9. Blach, J.K.; Bradley, B.A.; Abatzoglou, J.T.; Nagy, R.C.; Fusco, E.J.; Mahood, A.L. Human-started wildfires expand the fire niche across the United States. *Proc. Natl. Acad. Sci. USA* **2017**, *114*, 2946–2951. [CrossRef] [PubMed]
10. Scott, J.H.; Gilbertson-Day, J.W.; Moran, C.; Dillon, G.K.; Short, K.C.; Vogler, K.C. *Wildfire Risk to Communities: Spatial Datasets of Landscape-Wide Wildfire Risk Components for the United States*; Forest Service Research Data Archive: Fort Collins, CO, USA, 2020. [CrossRef]
11. LANDFIRE. Existing Vegetation Type Layer, LANDFIRE 2.0.0, U.S. Department of the Interior, Geological Survey, and U.S. Department of Agriculture. 2020. Available online: http://landfire.cr.usgs.gov/viewer/ (accessed on 1 July 2021).
12. Oliveira, S.; Rocha, J.; Sá, A. Wildfire risk modeling. *Curr. Opin. Environ. Sci. Health* **2021**, *23*, 100274. [CrossRef]
13. Smith, A.B. 2021 US Billion Dollar Weather and Climate Disasters in Historical Context including New County-Level Exposure, Vulnerability and Projected Damage Mapping. In Proceedings of the 102nd American Meteorological Society Annual Meeting, Houston, TX, USA, 23–27 January 2022; AMS: Providence, RI, USA, 2022.
14. Meldrum, J.R.; Barth, C.M.; Goolsby, J.B.; Olson, S.K.; Gosey, A.C.; White, J.; Brenkert-Smith, H.; Champ, P.A.; Gomez, J. Parcel-Level Risk Affects Wildfire Outcomes: Insights from Pre-Fire Rapid Assessment Data for Homes Destroyed in 2020 East Troublesome Fire. *Fire* **2022**, *5*, 24. [CrossRef]
15. Helmbrecht, D.; Gilbertson-Day, J.; Scott, J.H.; Hollingsworth, L. *Wildfire Risk to Residential Structures in the Island Park Sustainable Fire Community: Caribou-Targhee National Forest*; US Department of Agriculture, Forest Service, Fire Sciences Lab.: Missoula, MT, USA, 2016; 34p.
16. Glickman, D.; Babbitt, B. Urban Wildland Interface Communities within the Vicinity of Federal Lands That Are at High Risk from Wildfire. *Fed. Regist.* **2001**, *66*, 751–777.
17. Iglesias, V.; Stavros, N.; Balch, J.K.; Barrett, K.; Cobian-Iñiguez, J.; Hester, C.; Kolden, C.A.; Leyk, S.; Nagy, R.C.; Reid, C.E.; et al. Fires that matter: Reconceptualizing fire risk to include interactions between humans and the natural environment. *Environ. Res. Lett.* **2022**, *17*, 045014. [CrossRef]
18. Scott, J.H.; Short, K.C.; Finney, M.A. "FSim: The Large Fire Simulator Guide to Best Practices", Pyrologix LLC. Available online: https://pyrologix.com/wp-content/uploads/2019/11/FSimBestPractices_0.3.1.pdf (accessed on 5 March 2018).
19. Ott, C.W.; Adhikari, B.; Alexander, S.P.; Hodza, P.; Xu, C.; Minckley, T.A. Predicting fire propagation across heterogeneous landscapes using WyoFire: A Monte Carlo-driven wildfire model. *Fire* **2020**, *3*, 71. [CrossRef]
20. Lautenberger, C. Mapping Areas at Elevated Risk of Large-Scale Structure Loss Using Monte Carlo Simulation and Wildland Fire Modeling. *Fire Saf. J.* **2017**, *91*, 768–775. [CrossRef]
21. LFD: Landfire Fuel Dictionary. Available online: https://landfire.gov/DataDictionary/LF200/LF2016Remap_CC.pdf (accessed on 1 January 2020).

22. Finco, M.; Quayle, B.; Zhang, Y.; Lecker, J.; Megown, K.A.; Brewer, C.K. Monitoring Trends and Burn Severity (MTBS): Monitoring wildfire activity for the past quarter century using landsat data. In Proceedings of the Moving from Status to Trends: Forest Inventory and Analysis (FIA) Symposium 2012, Baltimore, MD, USA, 4–6 December 2012; Gen. Tech. Rep. NRS-P-105; U.S. Department of Agriculture, Forest Service, Northern Research Station: Newtown Square, PA, USA, 2012; pp. 222–228.
23. Miller, J.D.; Thode, A.E. Quantifying burn severity in a heterogeneous landscape with a relative version of the delta Normalized Burn Ratio (dNBR). *Remote Sens. Environ.* **2007**, *109*, 66–80. [CrossRef]
24. Hansen, M.C.; Potapov, P.V.; Moore, R.; Hancher, M.; Turubanova, S.A.; Tyukavina, A.; Thaus, D.; Stehmans, S.V.; Goetzt, J.S.; Loveland, T.R.; et al. High-Resolution Global Maps of 21st-Century Forest Cover Change. *Science* **2013**, *342*, 850–853. [CrossRef] [PubMed]
25. Scott, J.H.; Burgan, R.E. *Standard Fire Behavior Fuel Models: A Comprehensive Set for Use with Rothermel's Surface Fire Spread Model*; Gen. Tech. Rep. RMRS-GTR-153; U.S. Department of Agriculture, Forest Service, Rocky Mountain Research Station: Fort Collins, CO, USA, 2005; 72p.
26. Reeves, M.C.; Ryan, K.C.; Rollins, M.C.; Thompson, T.G. Spatial fuel data products of the LANDFIRE project. *Int. J. Wildland Fire* **2009**, *18*, 250–267. [CrossRef]
27. Martinuzzi, S.; Stewart, S.I.; Helmers, D.P.; Mockrin, M.H.; Hammer, R.B.; Radeloff, V.C. *The 2010 Wildland-Urban Interface of the Conterminous United States*; Research Map NRS-8; U.S. Department of Agriculture, Forest Service, Northern Research Station: Newtown Square, PA, USA, 2015; 124p. [CrossRef]
28. Krawchuk, M.A.; Moritz, M.A.; Parisien, M.A.; Dorn, J.V.; Hayhoe, K. Global Pyrogeography: The Current and Future Distribution of Wildfire. *PLoS ONE* **2009**, *4*, e5102. [CrossRef] [PubMed]
29. Bowman, D.M.J.S.; Kolden, C.A.; Abatzoglou, J.T.; Johnston, F.H.; van der Werf, G.R.; Flannigan, M. Vegetation fires in the Anthropocene. *Nat. Rev. Earth Environ.* **2020**, *1*, 500–515. [CrossRef]
30. LUCAS: Land Use and Carbon Scenario Simulator. Available online: https://www.usgs.gov/centers/western-geographic-science-center/science/lucas-model (accessed on 1 January 2020).
31. PRISM: Parameter-elevation Relationships on Independent Slopes Model. Available online: https://prism.oregonstate.edu/ (accessed on 1 January 2020).
32. Taylor, K.E.; Stouffer, R.J.; Meehl, G.A. An Overview of CMIP5 and the experiment design. *Bull. Amer. Meteor. Soc.* **2012**, *93*, 485–498. [CrossRef]
33. Abatzoglou, J.T.; Brown, T.J. A comparison of statistical downscaling methods suited for wildfire applications. *Int. J. Climatol.* **2012**, *32*, 772–780. [CrossRef]
34. Bates, P.D.; Niall, Q.; Chris, S.; Andrew, S.; Oliver, W.; Jeison, S.; James, S.; Gaia, O.; Jeff, N.; Guy, S.; et al. Combined Modeling of US Fluvial, Pluvial, and Coastal Flood Hazard Under Current and Future Climates. *Water Resour. Res.* **2021**, *57*, e2020WR028673. [CrossRef]
35. Kearns, E.J.; Amodeo, M.; Chadwick, S.; Eby, M.; Porter, J.R. Making Climate Change Personal: Enabling Action Through Communication of Flood Risk Science to Individuals. In Proceedings of the AGU Fall Meeting Abstracts, Online, 1–17 December 2020; Volume 2020, p. SY040-06.
36. Cohen, J.D. Reducing the wildland fire threat to homes: Where and how much? In Proceedings of the Symposium on Fire Economics, Planning, and Policy: Bottom Lines, San Diego, CA, USA, 5–9 April 1999; Gen. Tech. Rep. PSW-GTR-173; U.S. Department of Agriculture, Forest Service, Pacific Southwest Research Station: Albany, CA, USA, 1999; pp. 189–195.
37. Short, K.C. A spatial database of wildfires in the United States, 1992–2011. *Earth Syst. Sci. Data* **2014**, *6*, 1–27. [CrossRef]
38. Short, K.C. *Spatial Wildfire Occurrence Data for the United States, 1992–2018. [FPA_FOD_20210617]*, 5th ed.; Forest Service Research Data Archive: Fort Collins, CO, USA, 2021. [CrossRef]
39. Dillon, G.K.; Menakis, J.; Fay, F. Wildland Fire Potential: A Tool for Assessing Wildfire Risk and Fuels Management Needs. In Proceedings of the Large Wildland Fires Conference, Missoula, MT, USA, 19–23 May 2014; Proc. RMRS-P-73; Keane, R.E., Jolly, M., Parsons, R., Riley, K., Eds.; U.S. Department of Agriculture, Forest Service, Rocky Mountain Research Station: Fort Collins, CO, USA, 2015; pp. 60–76.
40. Silverman, B.W. *Density Estimation for Statistics and Data Analysis*; Chapman and Hall: New York, NY, USA, 1986.
41. Riley, K.L.; Abatzoglou, J.T.; Grenfell, I.C.; Klene, A.E.; Heinsch, F.A. The relationship of large fire occurrence with drought and fire danger indices in the western USA, 1984–2008: The role of temporal scale. *Int. J. Wildland Fire* **2013**, *22*, 894–909. [CrossRef]
42. Rehm, R.G.; McDermott, R.J. *Fire-Front Propagation Using the Level Set Method*; US Department of Commerce, National Institute of Standards and Technology: Gaithersburg, MD, USA, 2009; pp. 1–12.
43. Lautenberger, C. Wildland Fire Modeling with an Eulerian Level Set Method and Automated Calibration. *Fire Saf. J.* **2013**, *62*, 289–298. [CrossRef]
44. Finney, M.A.; McHugh, C.W.; Grenfell, I.C.; Riley, K.L.; Short, K.C. A simulation of probabilistic wildfire risk components for the continental United States. *Stoch. Environ. Res. Risk Assess.* **2011**, *25*, 973–1000. [CrossRef]
45. Parisien, M.A.; Dawe, D.A.; Miller, C.; Stockdale, C.A.; Armitage, O.B. Applications of simulation-based burn probability modeling: A review. *Int. J. Wildland Fire* **2019**, *28*, 913–926. [CrossRef]
46. Finney, M.A. *FARSITE, Fire Area Simulator–Model Development and Evaluation, No. 4*; US Department of Agriculture Forest Service, Rocky Mountain Research Station: Fort Collins, CO, USA, 1998.

47. Rothermel, R.C. *A Mathematical Model for Predicting Fire Spread in Wildland Fuels*; Research Paper Int-115; USDA Forest Service: Fort Collins, CO, USA, 1972.
48. Anderson, H.E. *Predicting Wind-Driven Wild Land Fire Size and Shape*; Research Paper INT-RP-305; United States Department of Agriculture Forest Service, Intermountain Forest and Range Experiment Station: Fort Collins, CO, USA, 1983.
49. Richards, G.D. A General Mathematical Framework for Modelling Two-Dimensional Wildland Fire Spread. *Int. J. Wildland Fire* **1995**, *5*, 63–72. [CrossRef]
50. Finney, M.A. Landscape fire simulation and fuel treatment optimization. In *Methods for Integrating Modeling of Landscape Change: Interior Northwest Landscape Analysis System*; US Department of Agriculture, Forest Service, Pacific Northwest Research Station: Portland, OR, USA, 2004; pp. 117–131.
51. Van Wagner, C.E. Conditions for the Start and Spread of Crown Fire. *Can. J. For. Res.* **1977**, *7*, 23–34. [CrossRef]
52. Cruz, M.G.; Alexander, M.E.; Wakimoto, R.H. Development and testing of models for predicting crown fire rate of spread in conifer forest stands. *Can. J. For. Res.* **2005**, *35*, 1626–1639. [CrossRef]
53. Sardoy, N.; Consalvi, J.L.; Kaiss, A.; Fernandez-Pello, A.C.; Porterie, B. Numerical study of ground-level distribution of firebrands generated by line fires. *Combust. Flame* **2008**, *154*, 478–488. [CrossRef]
54. Perryman, H.A.; Dugaw, C.J.; Varner, J.M.; Johnson, D.L. A cellular automata model to link surface fires to firebrand lift-off and dispersal. *Int. J. Wildland Fire* **2013**, *22*, 428–439. [CrossRef]
55. Sethian, J.A. A fast marching level set method for monotonically advancing fronts. *Proc. Natl. Acad. Sci. USA* **1996**, *93*, 1591–1595. [CrossRef]
56. First Street Foundation. The First National Flood Risk Assessment: Defining America's Growing Risk. 2020. Available online: https://assets.firststreet.org/uploads/2020/06/first_street_foundation__first_national_flood_risk_assessment.pdf (accessed on 8 August 2022).
57. Iowa State, Iowa Environmental Mesonet. 2022. Available online: https://mtarchive.geol.iastate.edu/ (accessed on 1 June 2022).
58. Torralba, V.; Doblas-Reyes, F.J.; Gonzalez-Reviriego, N. Uncertainty in recent near-surface wind speed trends: A global reanalysis intercomparison. *Environ. Res. Lett.* **2017**, *12*, 114019. [CrossRef]
59. Fang, G.H.; Yang, J.; Chen, Y.N.; Zammit, C. Comparing bias correction methods in downscaling meteorological variables for a hydrologic impact study in an arid area in China. *Hydrol. Earth Syst. Sci.* **2015**, *19*, 2547–2559. [CrossRef]
60. Luo, M.; Liu, T.; Meng, F.; Duan, Y.; Frankl, A.; Bao, A.; De Maeyer, P. Comparing bias correction methods used in downscaling precipitation and temperature from regional climate models: A case study from the Kaidu River Basin in Western China. *Water* **2018**, *10*, 1046. [CrossRef]
61. Switanek, M.B.; Troch, P.A.; Castro, C.L.; Leuprecht, A.; Chang, H.; Mukherjee, R.; Demaria, E.M.C. Scaled distribution mapping: A bias correction method that preserves raw climate model projected changes. *Hydrol. Earth Syst. Sci.* **2017**, *21*, 2649–2666. [CrossRef]
62. Gudmundsson, L.; Bremnes, J.B.; Haugen, J.E.; Engen-Skaugen, T. Technical Note: Downscaling RCM precipitation to the station scale using statistical transformations—A comparison of methods. *Hydrol. Earth Syst. Sci.* **2012**, *16*, 3383–3390. [CrossRef]